

Novel Vanilloid Receptor-1 Antagonists: 2. Structure–Activity Relationships of 4-Oxopyrimidines Leading to the Selection of a Clinical Candidate

Elizabeth M. Doherty,[†] Christopher Fotsch,[‡] Anthony W. Bannon,[§] Yunxin Bo,[†] Ning Chen,[†] Celia Dominguez, James Falsey,[†] Narender R. Gavva,[‡] Jodie Katon,[†] Thomas Nixey,[†] Vassil I. Ognyanov,[†] Liping Pettus,[†] Robert M. Rzasa,[†] Markian Stec,[†] Sekhar Surapaneni,[§] Rami Tamir,[‡] Jiawang Zhu,[†] James J. S. Treanor,[‡] and Mark H. Norman^{*,†}

Department of Chemistry Research and Discovery, Department of Neuroscience, and Department of Pharmacokinetics and Drug Metabolism, Amgen Inc., One Amgen Center Drive, Thousand Oaks, California 91320-1799

Received February 19, 2007

A series of novel 4-oxopyrimidine TRPV1 antagonists was evaluated in assays measuring the blockade of capsaicin or acid-induced influx of calcium into CHO cells expressing TRPV1. The investigation of the structure–activity relationships in the heterocyclic A-region revealed the optimum pharmacophoric elements required for activity in this series and resulted in the identification of subnanomolar TRPV1 antagonists. The most potent of these antagonists were thoroughly profiled in pharmacokinetic assays. Optimization of the heterocyclic A-region led to the design and synthesis of **23**, a compound that potentially blocked multiple modes of TRPV1 activation. Compound **23** was shown to be effective in a rodent “on-target” biochemical challenge model (capsaicin-induced flinch, ED₅₀ = 0.33 mg/kg p.o.) and was antihyperalgesic in a model of inflammatory pain (CFA-induced thermal hyperalgesia, MED = 0.83 mg/kg, p.o.). Based on its in vivo efficacy and pharmacokinetic profile, compound **23** (*N*-{4-[6-(4-trifluoromethyl-phenyl)-pyrimidin-4-yloxy]-benzothiazol-2-yl}-acetamide; AMG 517) was selected for further evaluation in human clinical trials.

Introduction

Vanilloid receptor-1 (TRPV1 or VR1), a well-characterized member of the transient receptor potential family of ion channels, has been implicated in the transmission of pain signaling. For this reason, the in vivo pharmacological effect of small molecule antagonists of TRPV1 has been the subject of intense investigations among many pain research groups.¹ This report is the second in a series describing the in vitro and in vivo properties of a novel class of pyrimidine TRPV1 antagonists discovered in our laboratories.^{2,3}

Our general approach for developing the structure–activity relationships (SAR) within this series was to dissect the pharmacophore into three regions (A, B, and C; Figure 1) and to optimize each region in a systematic fashion. In our first report, we discussed modifications to region B, which led to the identification of 4-oxopyrimidine **1**, a potent inhibitor that blocks capsaicin-induced ⁴⁵Ca²⁺ influx in rat and human TRPV1-expressing CHO cells with IC₅₀ values of 7.4 nM and 3.7 nM, respectively. While compound **1** was shown to be efficacious at blocking an on-target TRPV1-mediated response in vivo in the capsaicin-induced hypothermia model in rats, it did not show significant efficacy in the complete Freund's adjuvant (CFA)-induced inflammatory pain model. We postulated that the minimal effect observed in the pain model may be due to a combination of insufficient intrinsic TRPV1 potency and inadequate exposure in vivo. Therefore, at this stage of our SAR investigations, we sought to improve not only the potency of the 4-oxopyrimidine TRPV1 antagonists, but also to enhance their pharmacokinetic properties in vivo.

As an initial step toward improving the overall profile of these antagonists, we examined compound **1** in more detail. While

compound **1** demonstrated acceptable metabolic stability in rat liver microsomes (RLM CL_{in vitro} = 111 μL/min/mg) and good in vivo pharmacokinetic properties in rats (*t*_{1/2} = 2.8 h, CL_{in vivo} = 1.2 L/h/kg, *F*_{oral} = 31% at 5 mg/kg), measurements of stability in human liver microsomes (HLM CL_{in vitro} = 250 μL/min/mg) suggested that this compound would be extensively metabolized in humans. Further studies of compound **1** revealed the region of the molecule that was most susceptible to metabolism. Upon incubation of compound **1** with human liver microsomes in the presence of NADPH, only two oxidative metabolites were found (**M1** and **M2**; Figure 1). Although the exact sites of oxidation were not ascertained, analysis by MS/MS indicated that both metabolites were the result of mono-oxidation on the quinoline ring, while the center pyrimidine core and the trifluoromethyl phenyl moieties were unaffected. Therefore, our strategy to increase metabolic stability, as well as enhance potency in this series, was to systematically explore alternative heterocycles as replacements for the quinoline ring found in compound **1** (exemplified by generic structure **2**; Figure 1). This report describes the SAR investigations of the A-region, which culminated in the identification of our first TRPV1 clinical candidate, AMG 517 (*N*-{4-[6-(4-trifluoromethyl-phenyl)-pyrimidin-4-yloxy]-benzothiazol-2-yl}-acetamide; compound **23**). In the subsequent report, we will describe modifications made to the C-region that resulted in improvements in the pharmacokinetic and solubility profile of AMG 517.

Chemistry

Analogues of compound **1** were prepared by one of four general methods (methods A–D; Scheme 1). In method A, 4-chloro-6-[4-(trifluoromethyl)phenyl]-pyrimidine (**3**) was reacted with the alkoxide prepared by treatment of the requisite heteroaromatic alcohol (ArOH) with sodium hydride, as previously described.² The reactions were followed by HPLC or TLC and stirred at room temperature or heated until complete. In method B, the products were obtained by first converting 4-chloro-6-[4-(trifluoromethyl)phenyl]-pyrimidine (**3**) to the

* To whom correspondence should be addressed. Tel.: 805-447-1552. Fax: 805-480-3015. E-mail: markn@amgen.com.

[†] Department of Chemistry Research and Discovery.

[‡] Department of Neuroscience.

[§] Department of Pharmacokinetics and Drug Metabolism.

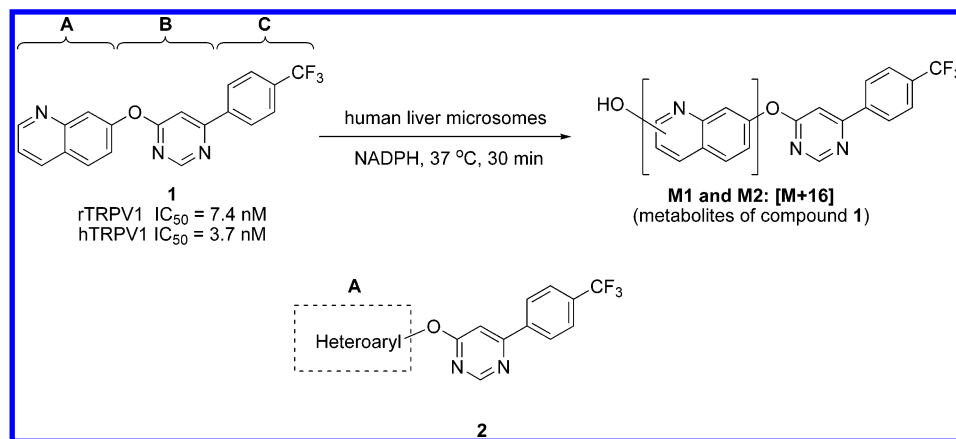
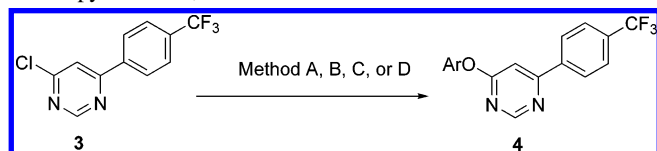


Figure 1. Lead compound **1**, oxidative metabolites of compound **1**, and generic SAR target **2**.

Scheme 1. General Methods for the Synthesis of 4-Oxypyrimidines, **4**^a



^a Method A: ArOH, NaH, DMF, 25 °C or heat. Method B: KF, DMSO, 120 °C; ArOH, K₂CO₃, DMF, 25 °C or 60 °C. Method C: ArOH, K₂CO₃, DMSO, 80–90 °C. Method D: ArOH, DBU, CH₃CN, reflux.

corresponding fluoropyrimidine intermediate and then treating this intermediate with various heteroaromatic alcohols in the presence of solid potassium carbonate in DMSO at 25 °C or 60 °C. In the third general procedure, method C, 4-chloro-6-[4-(trifluoromethyl)phenyl]-pyrimidine (**3**) was reacted directly with the heteroaromatic alcohol in the presence of a base (solid K₂CO₃) in DMSO at 80–90 °C. Finally, method D provided the target compounds (**4**) by conducting the reactions in refluxing acetonitrile, with DBU acting as the base.

With the exception of six examples described herein, the requisite heteroaromatic alcohols were either commercially available or readily prepared following published methods. To obtain the six heteroaromatic alcohols needed to complete the series (**6**, **7**, **10**, **14**, **18**, and **19**), the reaction sequences shown in Scheme 2 were followed. For example, treatment of commercially available 2-chloroquinolin-8-ol (**5**) with methylamine or dimethylamine under microwave heating provided 2-(methylamino)quinolin-8-ol (**6**) and 2-(dimethylamino)quinolin-8-ol (**7**), respectively (Scheme 2; eq I). For the preparation of 2-amino-8-hydroxyquinazoline (**10**), 3-methoxy-2-nitrobenzaldehyde (**8**) was reduced to 2-amino-3-methoxybenzaldehyde (**9**) using Fe(0) and NH₄Cl (Scheme 2; eq II). Condensation of aminobenzaldehyde **9** with guanidine in decalin at 190 °C, followed by deprotection of the phenol with NaSEt, afforded compound **10** in 48% yield. Aminoquinazolin-5-ol (**14**) was prepared in five steps starting from 2-amino-3-nitrophenol (**11**; Scheme 2; eq III). Protection of phenol **11** by methylation, followed by reduction of the nitro group with iron, provided the corresponding diaminobenzene. This free base was unstable upon standing and, therefore, was immediately converted to the more stable hydrogen sulfate salt **12**. Condensation of aniline **12** with ethyl glyoxylate provided an isomeric mixture of quinoxalinones from which the desired 8-methoxy-1*H*-quinoxalin-2-one (**13**) was isolated by silica gel chromatography. Quinoxalinone **13** was converted to 3-aminoquinoxalin-5-ol (**14**) by first generating the chloroquinoxaline intermediate using POCl₃, then introducing the amino group by treatment with NH₄-OH and CuI under microwave heating, and finally deprotecting

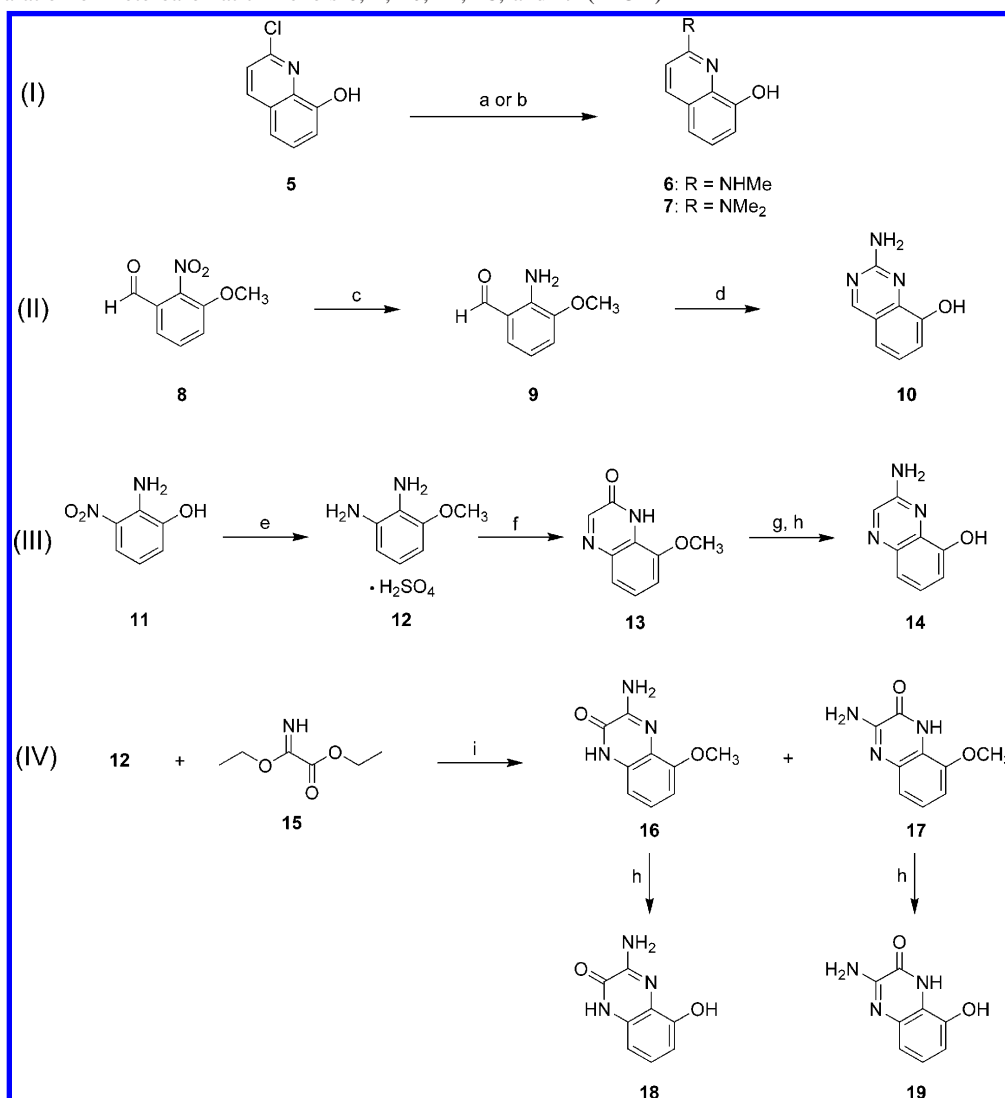
the phenol with AlCl₃. Intermediate diaminobenzene **12** was also used to prepare the requisite isomeric quinoxalinones **18** and **19** (Scheme 2; eq IV). In this case, diaminobenzene **12** was condensed with ethoxy-imino-acetic acid ethyl ester under conditions first described by Hermecz and co-workers⁴ to provide a 1.7 to 1 mixture of isomeric quinoxalinones **16** and **17**. The two isomers were separated by silica gel chromatography and independently deprotected with AlCl₃ to afford 3-amino-5-hydroxy-1*H*-quinoxalin-2-one (**18**) and 3-amino-8-hydroxy-1*H*-quinoxalin-2-one (**19**).

The final five compounds needed for this investigation required additional modifications following the initial heteroaromatic alcohol coupling (compounds **22**–**26**; Scheme 3). Treatment of the 2-aminoquinoline derivative **20** (prepared by method A, Scheme 1) with neat acetic anhydride at 105 °C provided the corresponding acylated analogue **22** in good yield. Similarly, 2-aminobenzothiazole derivative **21** (prepared by method C, Scheme 1) was acylated with either acetic anhydride, propionyl chloride, or isobutyl chloride to provide the corresponding amides **23**, **24** and **25**. The final compound, *N*-methylamide **26**, was prepared by the reaction of compound **23** with methyl iodide and sodium hydride in DMF at 0 °C.

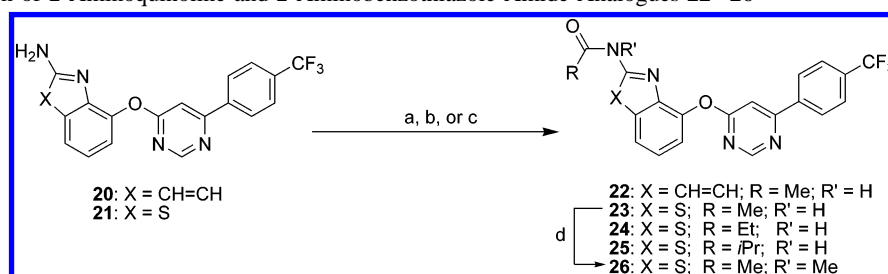
Results and Discussion

Structure–Activity Relationships (SAR). The compounds described were tested for their ability to block the capsaicin (CAP, 500 nM) or acid- (pH 5.0) induced uptake of ⁴⁵Ca²⁺ in CHO cells expressing rat TRPV1 (rTRPV1), as previously described.² Functional activity is reported as $IC_{50} \pm SEM$ (nM) in Tables 1–3. In a separate agonist assay, none of the compounds presented showed agonist activity. Results for all in vitro activities are the average of at least two independent experiments, with three replicates at each concentration.

In our previous studies of the cinnamides series of TRPV1 antagonists,⁵ we found that the 7-quinolinyl moiety imparted superior antagonist activity;⁶ however, this observation was based on a limited set of 6,6-fused heteroaromatic groups examined. Therefore, to more completely probe the heterocycle-receptor interactions in the A-region, we systematically examined each position of the nitrogen by surveying all possible quinoline and isoquinoline isomers in the 4-oxypyrimidine series (**27a–f** and **28a–g**, Table 1). When the nitrogen was moved around the ring, TRPV1 inhibitory activity decreased to varying degrees in both series. We found that the derivatives that contained the nitrogen in the 8-position gave the best results regardless of whether the ether linkage was attached to the 1- or 2-position of the quinoline ring (compounds **28a** and **1**, respectively).

Scheme 2. Preparation of Heteroaromatic Phenols **6**, **7**, **10**, **14**, **18**, and **19** (ArOH)^a

^a Reagents and conditions: (a) H₂NMe, dioxane, microwave, 200 °C; (b) HNMe₂, dioxane, microwave, 200 °C; (c) Fe(0), H₂O, MeOH, 60 °C; (d) guanidine hydrochloride, Na₂CO₃, decalin, 190 °C; EtSNa, DMF, reflux; (e) MeI, K₂CO₃, DMF, 25 °C; Fe(0), 12 M HCl, EtOH, H₂O, reflux; H₂SO₄; (f) EtOH, NaHCO₃, (HCO)CO₂Et, reflux; (g) POCl₃, coned NH₄OH, CuI, microwave, 140 °C; (h) AlCl₃, benzene, reflux; (i) EtOH, H₂O, NaHCO₃, 25 °C.

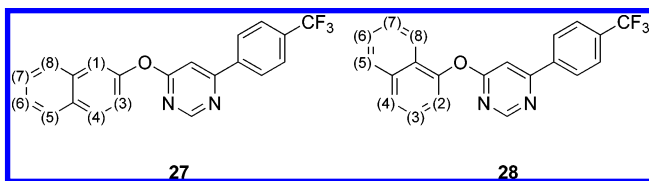
Scheme 3. Preparation of 2-Aminoquinoline and 2-Aminobenzothiazole Amide Analogues **22–26**^a

^a Reagents and conditions: (a) Ac₂O, 105 °C; (b) propionyl chloride, BEMP resin, THF, room temperature, 16 h; (c) isobutyryl chloride, BEMP resin, THF, room temperature, 16 h; (d) NaH, CH₃I, DMF, 0 °C.

While the 7-quinolinyl analogue **1** and the 8-quinolinyl analogue **28a** were approximately equipotent in the capsaicin-mediated assay, the 8-quinolinyl analogue was significantly less potent in the acid-mediated assay. Presumably, the binding region on the receptor is subtly changed at pH 5.0, resulting in the observed difference in activity.⁷ Despite an undesired reduction in activity in the acid-mediated assay,⁸ the 8-quinolinyl isomer **28a** demonstrated an encouraging improvement in microsomal stability over compound **1**. Specifically, in isolated rat and human liver microsomes, compound **28a** was cleared

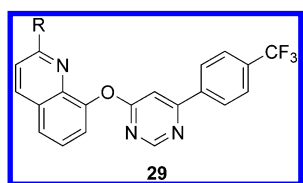
at rates of 44 and 135 $\mu\text{L}/\text{min}/\text{mg}$, respectively, compared to 111 and 250 $\mu\text{L}/\text{min}/\text{mg}$ for compound **1**. Therefore, we focused our continued efforts on improving the potency and pharmacokinetic properties of the 8-quinolinyl analogue.

It has been our experience that subtle modifications to the A-ring heterocycle can impact activity in the TRPV1 acid-mediated assay. Therefore, an initial set of compounds was prepared to investigate the effect of an additional substituent on the 2-position of the quinoline ring of compound **28a** (Table 2). The oxygen-substituted analogues (2-hydroxyquinoline, **29a**,

Table 1. Inhibition of CAP- (500 nM) and Acid- (pH 5.0) Induced $^{45}\text{Ca}^{2+}$ Influx into rTRPV1-Expressing CHO Cells for Compounds **1**, **27a–f**, and **28a–g**


cmpd	nitrogen position	rTRPV1 (CAP) IC ₅₀ (nM) ^a	rTRPV1 (acid) IC ₅₀ (nM) ^a
1	8	7.4 ± 1.0	8.0 ± 6.0
27a	7	460 ± 50	>4000
27b	6	1400 ± 200	>4000
27c	5	>4000	>4000
27d	4	>4000	>4000
27e	3	630 ± 30	>4000
27f	1	730 ± 100	>4000
28a	8	15 ± 7	>4000
28b	7	150 ± 20	120 ± 40
28c	6	120 ± 10	>4000
28d	5	660 ± 240	>4000
28e	4	>4000	>4000
28f	3	2900 ± 1000	>4000
28g	2	>4000	>4000

^a Each IC₅₀ value reported represents an average of at least two independent experiments with three replicates at each concentration (±SEM).

Table 2. Inhibition of CAP- (500 nM) and Acid- (pH 5.0) Induced $^{45}\text{Ca}^{2+}$ Influx into rTRPV1-Expressing CHO Cells for Compounds **28a**, **29a–d**, **20**, and **22**


cmpd	R	rTRPV1 (CAP) IC ₅₀ (nM) ^a	rTRPV1 (acid) IC ₅₀ (nM) ^a
28a	H	15 ± 7	>4000
29a	OH	>4000	>4000
29b	OMe	>4000	>4000
20	NH ₂	11 ± 6.5	62 ± 34
29c	NHMe	35 ± 2	43 ± 4
29d	NMe ₂	>4000	>4000
22	NHAc	77 ± 65	15 ± 18

^a Each IC₅₀ value reported represents an average of at least two independent experiments with three replicates at each concentration (±SEM).

and 2-methoxyquinoline, **29b**) proved to be significantly less potent in both assays. In contrast, the results for the nitrogen-substituted derivatives were more promising. For example, activity in the acid-mediated assay was restored with the 2-amino (**20**), 2-methylamino (**29c**), and 2-*N*-acetylamino (**22**) derivatives. However, activity was diminished when the quinoline was substituted in the 2-position with dimethylamino (**29d**). Taken together, these results suggest that the NH groups of **20**, **29c**, and **22** may act as hydrogen-bond donors to create a favorable interaction with the receptor under the conditions of both the capsaicin and the acid-mediated assays. This favorable interaction is eliminated in the case of the 2-methoxy and 2-dimethylamino substitutions (**29b** and **29d**, respectively). Furthermore, given that the 2-hydroxy derivative **29a** is likely to exist primarily in the quinolin-2-one tautomeric form,⁹ it may be less active than **20**, **29c**, and **22** because it cannot provide a similar hydrogen-bonding interaction in the 2-position.

From this initial set of 2-substituted quinolines, the 2-amino analogue **20** was selected for further SAR development. To examine this derivative in more detail, we conducted metabolism identification studies to obtain information regarding possible ways to further reduce clearance. As observed with compound **1**, the center pyrimidine core and the trifluoromethyl phenyl moieties of compound **20** were stable in human liver microsomes, but oxidative metabolism occurred on the quinoline ring. Studies in isolated rat and human hepatocytes¹⁰ showed that compound **20** underwent phase I and phase II metabolism, resulting in the formation of at least 15 metabolites. Consistent with the microsomal studies, the predominant site of metabolism in hepatocytes was the aminoquinoline ring (Figure 2). Hydroxylation on the quinoline ring, followed by sulfation, accounted for 70% of metabolism in rat hepatocytes.

With this information in hand, we prepared a series of analogues designed to block the proposed sites of metabolism, focusing initially on the 2-aminopyridyl portion of **20** (Table 3). The 2-amino-8-quinazolinyl analogue (**30**) was prepared to determine if an additional nitrogen atom introduced at the 3-position of the quinoline ring would serve to block metabolic oxidation. This modification resulted in the desired decrease in microsomal clearance, however, compound **30** suffered from a significant reduction in potency in the acid-mediated assay. Introduction of a nitrogen to the 4-position to afford 2-amino-8-quinoxalinyll analogue **31** gave the desired improvement in microsomal clearance without the attendant reduction in potency in the acid-mediated assay observed for compound **30**. Nevertheless, compound **31** demonstrated unacceptably high clearance in vivo [CL_{in vivo} = 4.3 L/h/kg], greater than the rate of rat hepatic blood flow. Despite this result, additional studies were conducted on **31**, which provided insights leading to further specific structural modifications. For example, compound **31**, dosed at 3 mg/kg, p.o., blocked 100% of the capsaicin-induced hypothermic response in our on-target in vivo telemetry model² (data not shown). This in vivo effect was surprising given the compound's high clearance and modest potency and led us to postulate that the in vivo activity observed for **31** was due to the formation of an active metabolite. Literature precedent¹¹ indicated that hydroxylation of the 3-position of the 2-amino-quinoxaline was likely, and for this reason, we prepared the corresponding oxidized derivative of **31** for further evaluation. The putative metabolite, compound **32**, demonstrated not only the anticipated improvement in clearance in the rat (CL_{in vivo} = 0.26 L/h/kg) but also a dramatic improvement in potency (IC₅₀ = 0.64 nM in the capsaicin assay, and IC₅₀ = 0.57 nM in the pH 5.0 assay).

Based on the results for **30** and **31**, it was clear that replacement of a single aromatic CH with nitrogen in the pyridinyl portion of the quinoline ring was insufficient to block the metabolism of **20**. Therefore, the 2-aminobenzothiazole analogue **21** was designed to block two of the proposed metabolic hot spots on the quinoline ring of **20**, replacing the C3–C4 atoms with sulfur. This modification resulted in a dramatic improvement in the metabolic stability in human liver microsomes (CL_{in vitro} < 5 μL/min/mg). In addition, compound

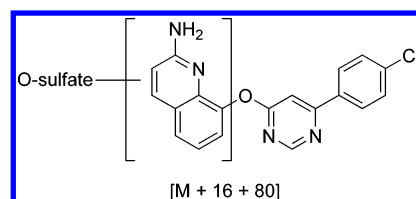
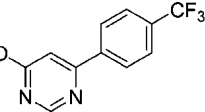
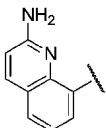
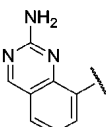
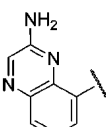
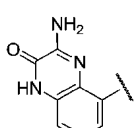
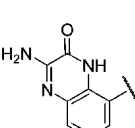
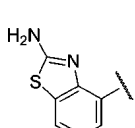
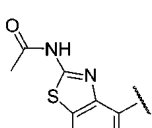
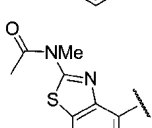
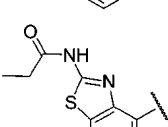
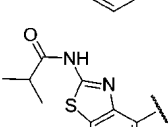
**Figure 2.** Major metabolites of compound **20** in rat hepatocytes.

Table 3. Inhibition of CAP- (500 nM) and Acid- (pH 5.0) Induced $^{45}\text{Ca}^{2+}$ Influx into rTRPV1-Expressing CHO Cells and In Vitro and In Vivo Clearance Data for Analogues of **20**

<div>Heterocycle-O-</div>						
Compound No.	Heterocycle	rTRPV1 (CAP) IC ₅₀ (nM) ^a	rTRPV1 (acid) IC ₅₀ (nM) ^a	Clearance data		
				HLM (μL/min/mg) ^b	RLM (μL/min/mg) ^b	rat in vivo (L/h/kg) ^c
20		11 ± 6.5	62 ± 34	183	110	1.2
30		14 ± 3	>4000	<14	38	1.5
31		63 ± 18	16 ± 0.3	<14	15	4.3
32		0.64 ± 0.04	0.57 ± 0.06	<14	<14	0.26
33		>4000	>4000	—	—	—
21		1.2 ± 0.9	>4000	<5	47	0.22
23		0.9 ± 0.8	0.5 ± 0.2	<5	50	0.25
26		>4000	860 ± 340	—	—	—
24		1100 ± 200	1500 ± 300	—	—	—
25		>4000	>4000	—	—	—

^a Each IC_{50} value reported represents an average of at least two independent experiments with three replicates at each concentration ($\pm\text{SEM}$).^b Rat liver microsomal (RLM) and human liver microsomal (HLM) clearance. ^c Intravenous bolus injection, 1 mg/kg in DMSO, $n = 2$ male Sprague-Dawley rats.

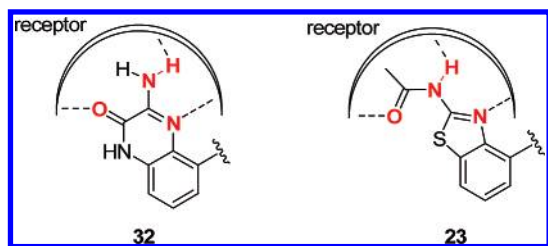


Figure 3. Binding elements required for optimum potency in the A-region (compounds **32** and **23**).

Table 4. Inhibition of CAP- (500 nM), Acid- (pH 5.0), or Heat-(45 °C) Induced $^{45}\text{Ca}^{2+}$ Influx into Human TRPV1-expressing CHO Cells for Compounds **23** and **32**.

cmpd	hTRPV1 (CAP) IC ₅₀ (nM) ^a	hTRPV1 (acid) IC ₅₀ (nM) ^a	hTRPV1 (heat) IC ₅₀ (nM) ^a
23	0.76 ± 0.4	0.62 ± 0.27	1.3 ± 0.1
32	0.8 ± 0.28	0.9 ± 0.35	0.4 ± 0.06

^a Each IC₅₀ value reported represents an average of at least two independent experiments with three replicates at each concentration (±SEM).

21 showed a 10-fold improvement in potency over **20** in the capsaicin-mediated assay (IC₅₀ = 1.2 nM vs 11 nM); however, activity in the acid-mediated assay was sacrificed (IC₅₀ > 4000 nM). In contrast, the *N*-acylated analogue **23** retained potency in both assays (IC₅₀ = 0.9 and 0.5 nM in the capsaicin- and acid-mediated assays, respectively), while also maintaining excellent metabolic stability in human liver microsomes (CL_{in vitro} < 5 μL/min/mg).

Based on the overall SAR and the two exquisitely potent TRPV1 antagonists identified (i.e., **23** and **32**), a pharmacophore model was constructed for the A-region of this series. The proposed hydrogen-bond donor–acceptor interactions between the carbonyl oxygen, NH proton, and the aromatic nitrogen of the antagonists and the receptor for both **23** and **32** are shown in Figure 3. The orientation of these elements seems to be critical for optimum potency, as evidenced by the significant reduction in potency observed for the isomeric analogue of **32** (compound **33**). In addition, when the amide NH of compound **23** was methylated (e.g., compound **26**), key interactions with the receptor were disrupted that also resulted in lower potency. The reduction in potency for the *N*-methylated compound (**26**) may be due to the elimination of the hydrogen-bonding interaction of the NH or due to an unfavorable conformational change in the acetyl group. Finally, the size of the pocket in this region of the receptor also appears to be sensitive to steric bulk. For example, significant decreases in TRPV1 inhibitory activity were observed when the alkyl group of the amide was extended further into the pocket, as in the case of the ethyl and isopropyl derivatives (**24** and **25**, respectively).

In addition to being tested at the rat TRPV1 receptor, compounds **23** and **32** were evaluated at the human TRPV1

receptor against three modes of activation (capsaicin, low pH, and heat). The results shown in Table 4 confirm that compounds **23** and **32** are potent inhibitors of the human TRPV1 under every condition tested.

To select a suitable clinical candidate, we compared some of the pharmacokinetic and physicochemical properties for the two most potent compounds in the series, **23** and **32** (Table 5). In our preliminary pharmacokinetic studies, the compounds were dosed at 1 mg/kg i.v. and plasma samples were collected and analyzed up to an 8-hour time point. In these studies, both compounds demonstrated long half-lives (*t*_{1/2}), low plasma clearance (CL), and high volumes of distribution (*V*_{ss}). However, when administered orally as a suspension at 3 mg/kg, compound **23** proved to be the superior candidate in terms of bioavailability, *F*_{oral} = 32%. In comparison, the oral bioavailability of **32** in rats was lower (*F*_{oral} = 7%, 5 mg/kg). While the aqueous solubility was low for both compounds,¹² the melting point of **32** was 115 degrees higher than **23**. The higher melting point of **32** and the resulting high-energy barrier to dissolution may help to explain the differences in oral bioavailability observed between **32** and **23**. Furthermore, compound **32** showed dose-limiting exposure at higher doses in rats (30 and 300 mg/kg, p.o.), presumably due to solubility-limited absorption. Conversely, compound **23** exhibited excellent exposure levels at the same doses, making it the better candidate for further safety assessment studies in rodents.

With compound **23** selected as the lead candidate, its pharmacokinetic properties were more extensively examined (Table 6). For routine screening purposes, we had set an 8-hour duration for initial in vivo pharmacokinetics studies in rats. Because compound **23** exhibited a relatively high volume of distribution and low clearance, the calculated half-life from these preliminary studies was an underestimation. To capture the true elimination phase, an additional study was conducted in rats measuring blood levels beyond an estimated four half-lives. In this extended 72 h study, a more accurate half-life of 31 h was determined for compound **23**.

The comparative pharmacokinetic profile for compound **23** was examined in rats, dogs, and monkeys (Table 6). In all species examined, compound **23** exhibited low clearance and moderately high volumes of distribution with consequently long half-lives. Oral bioavailability among the three species tested ranged from 23 to 52%. The mean exposures (AUC) for compound **23** increased in a dose proportional manner in the dose range of 1–10 mg/kg in rats, dogs, and monkeys (Figure 4).

Human pharmacokinetic parameters were projected based on allometric scaling and are presented in Table 6. Based on the allometric projection, compound **23** was predicted to have a long half-life in humans (60–120 h). The projected half-life in humans was expected to result in a 4-fold accumulation at steady-state, based on a QD dosing regimen, with minimal peak-to-trough fluctuations and low variability.

Table 5. Pharmacokinetic and Physicochemical Profile for **23** vs **32**

cmpd	intravenous dosing ^a					human liver microsomal stability (μL/min/mg)	solubility ^d (μg/mL)			mp (°C)
	CL (mL/h/kg)	<i>t</i> _{1/2} (h)	AUC _{0–∞} (ng·h/mL)	<i>V</i> _{ss} (mL/kg)	<i>F</i> _{oral} (%)		HCl _{aq} (0.01 N)	PBS ^e	SIF ^f	
23	190	6.3	5400	1556	32 ^b	<5	<1	<1	6.6	219–221
32	197	6.0	5143	1688	7 ^c	26	<1	<1	9.2	334–335

^a Study in fed male Sprague–Dawley rats dosed at 1 mg/kg in DMSO with sampling time up to 6 h. *n* = 2 animals per study. Interanimal variability was less than or equal to 30%. ^b Study in fasted male Sprague–Dawley rats dosed at 3 mg/kg as a suspension in 5% Tween 80/Oraplast with sampling time up to 8 h. *n* = 2 animals. Interanimal variability was less than or equal to 30%. ^c Study in fasted male Sprague–Dawley rats dosed at 5 mg/kg as a suspension in 5% Tween 80/Oraplast with sampling time up to 8 h. *n* = 2 animals. Interanimal variability was less than or equal to 30%. ^d Thermodynamic solubility measured in a high-throughput automated format (ref 11). ^e Phosphate buffered saline, pH 7.4. ^f Simulated intestinal fluid, pH 6.8.

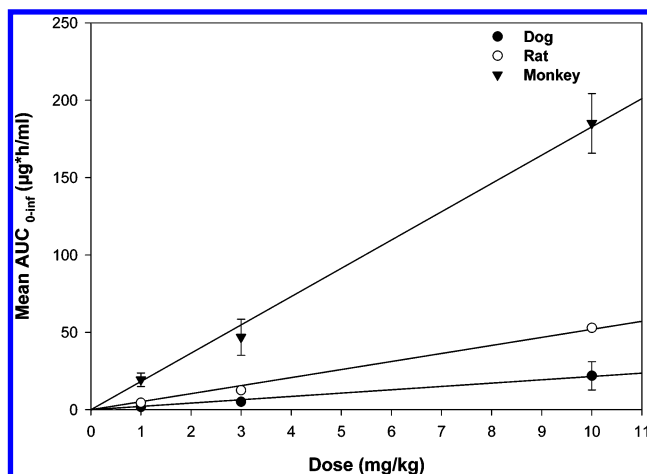


Figure 4. Dose linearity of **23** in rat, dog, and monkey at 1, 3, and 10 mg/kg, dosed p.o. as suspensions in 10% Pluronic/Oraplus.

In addition to the extensive in vivo pharmacokinetic studies, the on-target in vivo efficacy of **23** was measured in a capsaicin-induced flinching model in rats (Figure 5). The compound was dosed at 0, 0.1, 1, 3, 10, and 30 mg/kg as a suspension in 5% Tween 80 in Oraplus 1 h prior to capsaicin challenge. An ED_{50} = 0.35 mg/kg was calculated based on number of flinches per minute counted after intraplantar injection of capsaicin (0.5 µg in 5% EtOH/PBS). A significant correlation was found between number of flinches and plasma levels of compound, that is, the number of flinches decreased as plasma levels increased. Furthermore, we demonstrated that a 3 mg/kg dose (p.o.) of compound **23** significantly inhibited capsaicin-induced flinching up to 24 h. At 48 h, the animals behavior had returned to control levels.¹³ These results demonstrated that **23** was a potent inhibitor of TRPV1 in vivo.

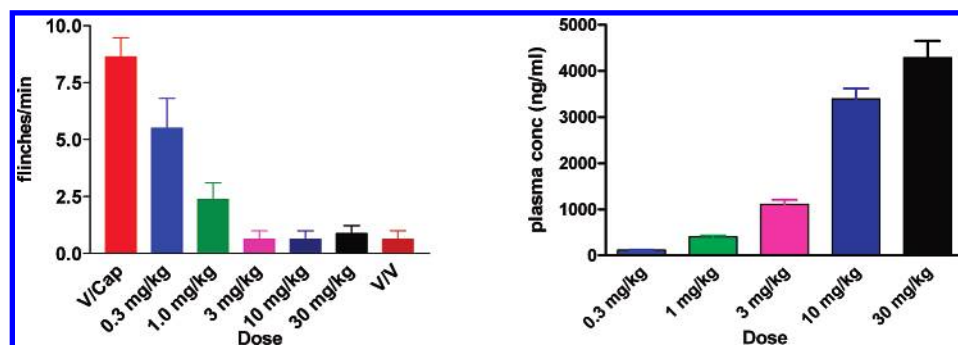


Figure 5. Efficacy and terminal plasma concentration of compound **23** in the capsaicin-induced flinch model (dosed p.o. in 5% Tween 80/Oraplus 1 h prior to capsaicin challenge; $n = 8$ per group of Harlan SD male rats).

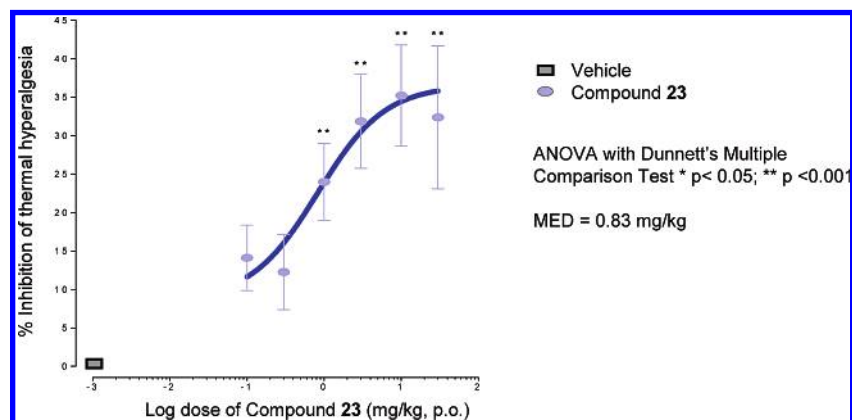


Figure 6. Dose-response for compound **23** in CFA-induced paw thermal hyperalgesia (dosed p.o. in 5% Tween 80/Oraplus; 21 h post-CFA treatment; $n = 14$ –35 per group of Harlan SD male rats).

Table 6. Mean Pharmacokinetic Parameters for Compound **23**

Following i.v. and p.o. Administration to Fasted Rat, Dog, and Monkey, with Projected Values for Human

species	intravenous dosing ^a				oral dosing ^b
	AUC _{0-∞} (ng·h/mL)	CL (mL/h/kg)	V _{ss} (mL/kg)	t _{1/2} (h)	F (%)
rat	8800	120	4000	31	51
dog	7400	140	7000	41	23
monkey	37 000	30	2300	62	52
human (projected)		50	4500	60–120	

^a 1 mg/kg in 80% PEG-400/H₂O, $n = 3$ animals per group. Variability for AUC_{0-∞}, CL, V_{ss}, and t_{1/2} values ranged from 7 to 38% for all species.

^b 1 mg/kg suspension in 10% Pluronic/Oraplus, $n = 3$ animals per group. Variability for F_{oral} ranged from 26 to 50% for all species.

Compound **23** was then evaluated for its ability to reverse thermal hyperalgesia in the CFA model in rats (Figure 6). The compound was dosed orally at 0.1, 0.3, 1, 3, 10, and 30 mg/kg to rats that had been treated 21 h in advance with CFA injected in the paw. Paw withdrawal latencies from a heat source were measured 3 h post-dosing with **23**. In this pain model, compound **23** showed dose-dependent inhibition of CFA-induced thermal hyperalgesia with efficacy at a minimum dose (MED) of 0.83 mg/kg (p.o.). The maximal effect observed in this model was approximately 35% of control at a dose of 10 mg/kg. In comparison, in the on-target model we observed a 100% return to control levels at 10 mg/kg (Figure 5), suggesting that the target is fully covered at this dose. Therefore, the degree of reversal of thermal hyperalgesia observed in the CFA model probably reflects the magnitude of involvement of TRPV1 in the CFA-induced inflammatory pain pathway in rodents.

Based on its excellent overall in vitro and in vivo profile, compound **23** was selected for further evaluation in human clinical trials and was designated AMG 517. Additional details of the pharmacological, toxicological, and clinical profiles of AMG 517 will be reported elsewhere.

Summary

In this investigation, we examined the structure–activity relationships in the heterocyclic A-region of the 4-oxypyrimidine TRPV1 antagonists, with the aim of improving potency and increasing metabolic stability of lead compound **1**. Through these SAR investigations, we developed several potent TRPV1 antagonists and increased our understanding of the pharmacophoric elements required in the A-ring. The initial set of quinoline and isoquinoline derivatives revealed that the 8-quinolinyl isomer (compound **28a**) retained TRPV1 potency in the capsaicin-mediated assay, while being more stable than compound **1** upon incubation in rat or human liver microsomes. Furthermore, we found that an additional potency-enhancing hydrogen-bonding interaction with the TRPV1 receptor could be obtained by substituting the 2-position of the quinoline ring with an amino group (e.g., compound **20**). Metabolite identification studies showed that compound **20** was extensively metabolized on the 2-aminoquinoline moiety. Attempts to block the metabolism of the quinoline ring led to the identification of two metabolically stable and exquisitely potent TRPV1 antagonists, benzothiazole **23** and quinoxalinone **32**. Further evaluation of compound **23** showed that it potently blocked multiple modes of TRPV1 activation and was effective in a rodent on-target biochemical challenge model (capsaicin-induced flinch, ED_{50} = 0.33 mg/kg p.o.). In the CFA pain model in rats, compound **23** showed a dose-dependent inhibition of thermal hyperalgesia (MED = 0.3 mg/kg, p.o.). Because of its excellent pharmacokinetic properties and in vivo efficacy, compound **23** (AMG 517) was selected for further evaluation in human clinical trials for the treatment of inflammatory pain. In part 3 of this series, we will describe modifications made to the C-region that resulted in improvements in the pharmacokinetic and solubility profile of AMG 517.

Experimental Section

Capsaicin-Induced Flinch Model. Male Sprague–Dawley rats (Charles River Laboratories (CRL), Wilmington, MA) weighing 250–300 g were used. Animals were allowed at least a 1 week acclimation period in Amgen's AAALAC-accredited animal care facility prior to being tested. On test day, animals were dosed (p.o.) with compound **23** at a dosing volume of 5 mL/kg 1 h prior to the administration of a capsaicin challenge. The vehicle for compound **23** was 5% Tween 80 in Oraplus. Capsaicin was administered at a dose of 0.5 μ g into the right paw of the animal. The injection volume for capsaicin was 25 μ L, and the vehicle for capsaicin was 5% EtOH in PBS (Ca^{++} and Mg^{++} free). Immediately following intraplantar injection of capsaicin, flinch responses were counted for a 1 min period. Investigators counting flinches were blinded to the treatment conditions. For each treatment group, n = 8. The ED_{50} value was computed using GraphPad Prism software (San Diego, CA). Significance level was set at p < 0.05. Percent inhibition was computed as $100 \times (1 - (\text{test value} - \text{mean vehicle/vehicle value})/(\text{mean vehicle/capsaicin value} - \text{mean vehicle/vehicle value}))$.

Chemistry. Unless otherwise noted, all materials were obtained from commercial suppliers and used without further purification. Anhydrous solvents were obtained from Aldrich or EM Science and used directly. All reactions involving air- or moisture-sensitive reagents were performed under a nitrogen or argon atmosphere.

All final compounds were purified to >95% purity, as determined by reverse-phase high-performance liquid chromatography (rp-HPLC). Purity was determined on an Agilent 1100 spectrometer by method A, Phenomenex Luna C₈ column (100 \times 4.6 mm, 5 μ) at 40 $^{\circ}$ C with a 1 mL/min flow rate using a gradient of 10–100% 0.1% TFA in acetonitrile in 0.1% TFA in water over 10 min; or method B, YMC ODS-AM C₁₈ column (100 \times 2.1 mm, 5 μ) at 40 $^{\circ}$ C with a 0.5 mL/min flow rate using a gradient of 10–100% 0.1% TFA in acetonitrile in 0.1% TFA in water over 7 min. Silica gel chromatography was performed using either glass columns packed with silica gel (200–400 mesh, Aldrich Chemical) or prepacked silica gel cartridges (Biotage or RediSep). Melting points were determined on a Buchi-545 melting point apparatus and are uncorrected. NMR spectra were determined with a Bruker 300 MHz or DRX 400 MHz spectrometer. Chemical shifts are reported in parts per million (ppm, δ units). Low-resolution mass spectral (MS) data were determined on a Perkin-Elmer-SCIEX API 165 mass spectrometer using electrospray (ES) ionization modes (positive or negative). High-resolution mass spectral (HRMS) data were determined on a 7T Bruker FTICR mass spectrometer using ES ionization mode (positive). Combustion analyses were performed by Atlantic Microlab, Inc., Norcross, GA, and were within 0.4% of calculated values unless otherwise noted.

General Methods for the Synthesis of 4-Oxypyrimidines (4).

Method A: In an oven-dried, round-bottomed flask, a solution of the alcohol (1.1 equiv) in DMF (0.15–0.25 M) was stirred at room temperature and treated portionwise with sodium hydride, as a 60% dispersion in mineral oil (1.2 equiv). Upon complete addition, the reaction mixture was stirred for 10 min and then 4-chloro-6-(4-(trifluoromethyl)phenyl)pyrimidine² (**3**; 1.0 equiv) was added in one portion. The reaction mixture was stirred at room temperature, or heated, until complete (as determined by TLC or HPLC). The reaction mixture was diluted with H₂O and extracted with EtOAc. The organic extract was washed successively with 1 N NaOH, H₂O, and satd NaCl, dried over Na₂SO₄, filtered, and concentrated in vacuo to afford the crude product.

Method B: To a solution of 4-chloro-6-(4-(trifluoromethyl)phenyl)pyrimidine (**3**; 2.0 g, 7.7 mmol) in DMSO (15 mL) was added potassium fluoride (3.6 g, 61 mmol). The mixture was stirred at 120 $^{\circ}$ C for 6 h. After cooling to room temperature, the mixture was poured into H₂O (200 mL) and extracted with EtOAc (2 \times 200 mL). The combined extracts were washed with H₂O (3 \times 200 mL) and satd NaCl (200 mL) and then dried over Na₂SO₄, filtered, and concentrated in vacuo onto silica gel. Purification by silica gel chromatography (gradient: 0 to 6% EtOAc in hexanes) afforded 4-fluoro-6-(4-(trifluoromethyl)phenyl)pyrimidine (1.7 g, 90%) as a white solid. MS (ESI, pos. ion) m/z : 243 (M + 1). ¹H NMR (400 MHz, CDCl₃) δ 7.39 (t, J = 1.0 Hz, 1 H), 7.80 (d, J = 8.4 Hz, 2 H), 8.21 (d, J = 8.4 Hz, 2 H), 9.02 (t, J = 1.0 Hz, 1 H).

To an oven-dried, round-bottomed flask was added 4-fluoro-6-(4-(trifluoromethyl)phenyl)pyrimidine (1.8 equiv), alcohol (1.0 equiv), K₂CO₃ (2.0 equiv), and DMF (0.08–0.15 M). The reaction mixture was stirred at room temperature, or at 60 $^{\circ}$ C, until complete (as determined by TLC or HPLC). The mixture was poured into aq NaHCO₃ and extracted with EtOAc. The extract was washed with H₂O and satd NaCl, dried over Na₂SO₄, filtered, and concentrated in vacuo to afford the crude product.

Method C: A mixture of **3** (1.1 equiv), alcohol (1.0 equiv), and solid K₂CO₃ (1.4–2.0 equiv) in anhydrous DMSO (0.1–0.5 M) or anhydrous DMF (0.1–0.5 M) was stirred in an 80–90 $^{\circ}$ C oil bath until complete (as determined by TLC or HPLC). The reaction mixture was allowed to cool to room temperature and diluted with EtOAc. The mixture was washed with H₂O and satd NaCl, dried over MgSO₄, filtered, and concentrated in vacuo to afford the crude product.

Method D: A suspension of the alcohol (1.2 equiv) in CH₃CN (0.05–0.1 M) was treated with 1,8-diazabicyclo[5.4.0]undec-7-ene (1.2 equiv) followed by **3** (1.0 equiv). The reaction mixture was stirred at reflux until complete (as determined by TLC or HPLC). The mixture was allowed to cool to room temperature and concentrated in vacuo to afford the crude product.

8-(6-(4-(Trifluoromethyl)phenyl)pyrimidin-4-yloxy)quinolin-2-amine (20). Following method A, 2-amino-8-quinolinol (0.70 g, 4.4 mmol) and **3** (1.2 g, 4.6 mmol), after purification of the crude product by silica gel chromatography (98:2 CH₂Cl₂/2 M NH₃ in MeOH), followed by recrystallization from CH₂Cl₂ and hexane, afforded **20** (1.0 g, 60%) as fine white crystals. Mp: 203–204 °C. MS (ESI, pos. ion) *m/z*: 383 (M + 1). ¹H NMR (400 MHz, DMSO-*d*₆) δ 6.44 (s, 2 H), 6.77 (d, *J* = 8.9 Hz, 1 H), 7.20 (t, *J* = 7.8 Hz, 1 H), 7.38 (dd, *J* = 1.3, 7.6 Hz, 1 H), 7.60 (dd, *J* = 1.3, 8.0 Hz, 1 H), 7.89 (d, *J* = 1.0 Hz, 1 H), 7.93 (d, *J* = 8.3 Hz, 2 H), 7.96 (d, *J* = 9.0 Hz, 1 H), 8.45 (d, *J* = 8.2 Hz, 2 H), 8.74 (d, *J* = 1.0 Hz, 1 H). Anal. (C₂₀H₁₃F₃N₄O): C, H, N, F.

4-[6-(4-(Trifluoromethyl-phenyl)-pyrimidin-4-yloxy)-benzothiazol-2-ylamine (21). Following method C, 2-amino-4-hydroxy-benzothiazole (0.42 g, 2.5 mmol) and **3** (0.97 g, 3.8 mmol), after purification of the crude product by silica gel chromatography (2:1 hexanes/EtOAc), provided **21** (0.77 g, 79%) as a white solid. Mp: 245–246 °C. MS (ESI, pos. ion) *m/z*: 389 (M + 1). ¹H NMR (400 MHz, CDCl₃) δ 5.23 (br s, 2 H), 7.16–7.25 (m, 2 H), 7.45 (s, 1 H), 7.55 (dd, *J* = 1.6, 7.8 Hz, 1 H), 7.77 (d, *J* = 7.8 Hz, 2 H), 8.18 (d, *J* = 7.8 Hz, 2 H), 8.84 (s, 1 H). Anal. (C₁₈H₁₁F₃N₄O₅): C, H, N, S.

N-{8-[6-(4-(Trifluoromethyl-phenyl)-pyrimidin-4-yloxy)-quinolin-2-yl]-acetamide (22). A mixture of **20** (0.79 g, 2.1 mmol) and acetic anhydride (2.5 mL, 2.6 mmol) was stirred in a 105 °C oil bath for 8 h. The volatiles were removed in vacuo to afford a solid residue. Purification of the crude product by silica gel chromatography (1:2 EtOAc/hexane) followed by recrystallization from EtOAc provided **22** (0.56 g, 63%) as a white solid. Mp: 204–206 °C. MS (ESI, pos. ion) *m/z*: 425 (M + 1). ¹H NMR (400 MHz, CDCl₃) δ 2.16 (s, 3 H), 7.49 (s, 1 H), 7.51–7.54 (m, 2 H), 7.74–7.80 (m, 3 H), 7.94 (s, 1 H), 8.22 (dd, *J* = 8.4, 10.4 Hz, 3 H), 8.77 (s, 1 H). Anal. (C₂₂H₁₅F₃N₄O₂): C, H, N.

N-{4-[6-(4-(Trifluoromethyl-phenyl)-pyrimidin-4-yloxy)-benzothiazol-2-yl]-acetamide (23). A mixture of **21** (97 mg, 0.25 mmol) and acetic anhydride (0.24 mL, 2.5 mmol) was stirred in a 105 °C oil bath for 8 h. The volatiles were removed in vacuo, and the solid residue was recrystallized from EtOAc in hexanes. The solid was dried in vacuo at 60 °C to give **23** (52 mg, 48%) as a white solid. Mp: 219–221 °C. MS (ESI, pos. ion) *m/z*: 431 (M + 1). ¹H NMR (400 MHz, DMSO-*d*₆) δ ppm 2.13 (s, 3 H), 7.35 (dd, *J* = 1.4, 7.8 Hz, 1 H), 7.39 (t, *J* = 7.8 Hz, 1 H), 7.87–7.96 (m, 3 H), 7.97 (d, *J* = 0.78 Hz, 1 H), 8.45 (d, *J* = 8.0 Hz, 2 H), 8.80 (d, *J* = 0.78 Hz, 1 H), 12.42 (s, 1 H). Anal. Calcd for C₂₀H₁₃F₃N₄O₂S·0.75H₂O: C, 54.11; H, 3.29; N, 12.62; S, 7.22. Found: C, 54.12; H, 3.07; N, 12.61; S, 7.30. HPLC analysis, method A: 98.2% at 215 nm; 99.5% at 254 nm; retention time 8.76 min.

N-{4-[6-(4-(Trifluoromethyl-phenyl)-pyrimidin-4-yloxy)-benzothiazol-2-yl]-propionamide (24). To a solution of **21** (0.19 g, 0.49 mmol) in THF (5 mL) was added propionyl chloride (87 μL, 1.0 mmol), followed by 2-*tert*-butylimino-2-diethylamino-1,3-dimethyl-perhydro-1,3,2-diazaphosphorine, polymer-bound (BEMP resin; 0.34 g, 0.75 mmol). The reaction mixture was stirred at room temperature for 16 h. The solid was removed by suction filtration and washed with CH₂Cl₂. The combined filtrate and washes were concentrated in vacuo to give a light-yellow solid. Purification by silica gel chromatography (1:4 EtOAc/hexane) provided **24** (0.047 g, 42%) as a white solid. Mp: 197–198 °C. MS (ESI, pos. ion) *m/z*: 445 (M + 1). ¹H NMR (400 MHz, CDCl₃) δ 1.26 (t, *J* = 8.0 Hz, 3 H), 2.47 (qt, *J* = 8.0 Hz, 2 H), 7.29 (dd, *J* = 1.0, 8.0 Hz, 1 H), 7.40 (t, *J* = 8.0 Hz, 1 H), 7.45 (d, *J* = 1.0 Hz, 1 H), 7.76–7.78 (m, 3 H), 8.18 (d, *J* = 8.0 Hz, 2 H), 8.80 (d, *J* = 1.0 Hz, 1 H), 8.90 (br s, 1 H). Anal. (C₂₁H₁₅F₃N₄O₂S): C, H, N, S.

N-(4-[6-(4-(Trifluoromethyl-phenyl)pyrimidin-4-yloxy)benzo[d]thiazol-2-yl)isobutyramide (25). According to the procedure described for the preparation of **24**, compound **21** (0.19 g, 0.49 mmol) and isobutyryl chloride (0.11 mL, 1.0 mmol), after purification of the crude product by silica gel chromatography (1:4 EtOAc/hexane), provided **25** (0.10 g, 45%) as a white solid. Mp: 178–181 °C. MS (ESI, pos. ion) *m/z*: 459 (M + 1). ¹H NMR (400 MHz, CDCl₃) δ 1.28 (d, *J* = 4.0 Hz, 6 H), 2.62 (dq, *J* = 4.0, 8.0 Hz, 1

H), 7.30 (dd, *J* = 1.0, 8.0 Hz, 1 H), 7.41 (t, *J* = 8.0 Hz, 1 H), 7.48 (d, *J* = 1.0 Hz, 1 H), 7.77–7.79 (m, 3 H), 8.20 (d, *J* = 8.0 Hz, 2 H), 8.82 (d, *J* = 1.0 Hz, 1 H), 9.18 (br s, 1 H). Anal. (C₂₂H₁₇F₃N₄O₂S): C, H, N, S.

N-Methyl-N-(4-(6-(4-(trifluoromethyl)phenyl)pyrimidin-4-yloxy)benzo[d]thiazol-2-yl)acetamide (26). A mixture of **23** (215 mg, 0.50 mmol) and iodomethane (31 μL, 0.50 mmol) in anhydrous DMF (2 mL) was treated with NaH (24 mg, 0.60 mmol) at 0 °C. The reaction mixture was stirred at 0 °C for 20 min, then quenched with satd NH₄Cl (10 mL) and extracted with EtOAc (2 × 30 mL). The combined organic extract was washed with H₂O (2 × 20 mL) and satd NaCl (20 mL), dried over Na₂SO₄, filtered, and concentrated in vacuo. Purification of the crude product by silica gel chromatography (30% EtOAc in hexane) provided **26** (140 mg, 63% yield) as a white solid. MS (ESI, pos. ion) *m/z*: 446 (M + 1). ¹H NMR (300 MHz, CDCl₃) δ 2.40 (s, 3 H), 3.57 (s, 3 H), 7.29 (dd, *J* = 1.2, 7.9 Hz, 1 H), 7.39 (t, *J* = 7.8 Hz, 1 H), 7.45 (d, *J* = 1.0 Hz, 1 H), 7.72–7.81 (m, 3 H), 8.20 (d, *J* = 8.0 Hz, 2 H), 8.82 (d, *J* = 1.0 Hz, 1 H). Anal. (C₂₁H₁₅F₃N₄O₂S): C, H, N.

7-(6-(4-(Trifluoromethyl)phenyl)pyrimidin-4-yloxy)isoquinoline (27a). Following method A, isoquinolin-7-ol (0.40 g, 2.8 mmol) and **3** (0.67 g, 2.6 mmol), after purification of the crude product by silica gel chromatography (gradient: 1–2% 2 M NH₃ in MeOH/CH₂Cl₂), afforded **27a** (0.35 g, 36%) as a tan solid. Mp: 167–168 °C. MS (ESI, pos. ion) *m/z*: 368 (M + 1). ¹H NMR (400 MHz, DMSO-*d*₆) δ 7.75 (dd, *J* = 2.4, 8.8, 1 H), 7.91 (d, *J* = 5.9 Hz, 1 H), 7.94 (d, *J* = 8.4 Hz, 2 H), 8.02 (s, 1 H), 8.04 (d, *J* = 2.2 Hz, 1 H), 8.11 (d, *J* = 9.0 Hz, 1 H), 8.47 (d, *J* = 8.2 Hz, 2 H), 8.55 (d, *J* = 5.7 Hz, 1 H), 8.89 (s, 1 H), 9.33 (s, 1 H). Anal. (C₂₀H₁₂F₃N₃O): C, H, N.

6-(6-(4-(Trifluoromethyl)phenyl)pyrimidin-4-yloxy)isoquinoline (27b). Following method B, isoquinolin-6-ol (0.060 g, 0.41 mmol) and **3** (0.18 g, 0.74 mmol), after purification of the crude product by silica gel chromatography (gradient: 10–50% EtOAc in hexanes), afforded **27b** (0.058 g, 39%) as an off-white solid. Mp: 195–196 °C. MS (ESI, pos. ion) *m/z*: 368 (M + 1). ¹H NMR (400 MHz, DMSO-*d*₆) δ 7.64 (dd, *J* = 2.3, 8.8 Hz, 1 H), 7.85 (d, *J* = 5.9 Hz, 1 H), 7.89 (d, *J* = 2.3 Hz, 1 H), 7.94 (d, *J* = 8.4 Hz, 2 H), 8.03 (d, *J* = 1.0 Hz, 1 H), 8.26 (d, *J* = 9.0 Hz, 1 H), 8.47 (d, *J* = 8.2 Hz, 2 H), 8.54 (d, *J* = 5.7 Hz, 1 H), 8.91 (d, *J* = 1.0 Hz, 1 H), 9.37 (s, 1 H). Anal. Calcd for C₂₀H₁₂F₃N₃O: C, 65.40; H, 3.29; N, 11.44. Found: C, 64.87; H, 3.27; N, 11.18.

6-(6-(4-(Trifluoromethyl)phenyl)pyrimidin-4-yloxy)quinoline (27c). Following method A, 6-hydroxyquinoline (0.11 g, 0.77 mmol) and **3** (0.20 g, 0.77 mmol), after purification of the crude product by silica gel chromatography (2:1 hexane/EtOAc), provided **27c** (0.14 g, 48%) as a white solid. Mp: 165–166 °C. MS (ESI, pos. ion) *m/z*: 368 (M + 1). ¹H NMR (400 MHz, CDCl₃) δ 7.43 (d, *J* = 1.2 Hz, 1 H), 7.47 (dd, *J* = 4.3, 8.2 Hz, 1 H), 7.59 (dd, *J* = 2.5, 9.2 Hz, 1 H), 7.67 (d, *J* = 2.7 Hz, 1 H), 7.80 (d, *J* = 8.2 Hz, 2 H), 8.18 (dd, *J* = 1.6, 8.2 Hz, 1 H), 8.22 (d, *J* = 8.2 Hz, 2 H), 8.23 (d, *J* = 9.0 Hz, 1 H), 8.89 (d, *J* = 1.2 Hz, 1 H), 8.96 (dd, *J* = 1.6, 4.3 Hz, 1 H). Anal. (C₂₀H₁₂F₃N₃O): C, H, N.

3-(6-(4-(Trifluoromethyl)phenyl)pyrimidin-4-yloxy)quinoline (27d). Following method A, quinolin-3-ol (0.15 g, 1.1 mmol) and **3** (0.30 g, 1.2 mmol), after recrystallization of the crude product from EtOAc in hexane, provided **27d** (0.25 g, 64%) as a white solid. Mp: 208–209 °C. MS (ESI, pos. ion) *m/z*: 368 (M + 1). ¹H NMR (400 MHz, DMSO-*d*₆) δ 7.69 (ddd, *J* = 1.2, 7.0, 8.0 Hz, 1 H), 7.81 (ddd, *J* = 1.4, 7.0, 8.5 Hz, 1 H), 7.95 (d, *J* = 8.2 Hz, 2 H), 8.03 (d, *J* = 7.8 Hz, 1 H), 8.08–8.12 (m, 2 H), 8.35 (d, *J* = 2.7 Hz, 1 H), 8.49 (d, *J* = 8.2 Hz, 2 H), 8.90 (d, *J* = 1.0 Hz, 1 H), 8.93 (d, *J* = 2.5 Hz, 1 H). Anal. (C₂₀H₁₂F₃N₃O·0.1H₂O): C, H, N.

3-(6-(4-(Trifluoromethyl)phenyl)pyrimidin-4-yloxy)isoquinoline (27e). Following method A, 3-hydroxyisoquinoline (1.6 g, 11 mmol) and **3** (3.9 g, 15 mmol), after purification of the crude product by silica gel chromatography (gradient: 1–2.5% 2 M NH₃ in MeOH/CH₂Cl₂), then repeat purification by silica gel chromatography (gradient: 0.5–1.8% 2 M NH₃ in MeOH/CH₂Cl₂), and washing the product with 10% EtOAc in hexane, afforded **27e** (0.10

g, 2.5%) as a tan solid. Mp: 157–160 °C. MS (ESI, pos. ion) m/z : 368 ($M + 1$). ^1H NMR (400 MHz, DMSO- d_6) δ 7.70 (ddd, $J = 1.0, 7.0, 8.0$ Hz, 1 H), 7.80 (s, 1 H), 7.84 (ddd, $J = 1.2, 7.0, 8.2$ Hz, 1 H), 7.93 (d, $J = 8.2$ Hz, 2 H), 7.99 (d, $J = 0.98$ Hz, 1 H), 8.03 (d, $J = 8.0$ Hz, 1 H), 8.22 (d, $J = 7.6$ Hz, 1 H), 8.46 (d, $J = 8.0$ Hz, 2 H), 8.91 (d, $J = 0.98$ Hz, 1 H), 9.23 (s, 1 H). Anal. ($\text{C}_{20}\text{H}_{12}\text{F}_3\text{N}_3\text{O} \cdot 0.1\text{H}_2\text{O}$): C, H, N.

2-(6-(4-(Trifluoromethyl)phenyl)pyrimidin-4-yloxy)quinoline (27f). Following method A, quinolin-2-ol (0.30 g, 2.1 mmol) and **3** (0.58 g, 2.2 mmol), after purification of the crude product by silica gel chromatography (40% EtOAc in hexanes), followed by recrystallization from 20% EtOAc/hexane, afforded **27f** (0.20 g, 26%) as a white solid. Mp: 145–149 °C. MS (ESI, pos. ion) m/z : 368 ($M + 1$). ^1H NMR (400 MHz, DMSO- d_6) δ 7.49 (d, $J = 8.6$ Hz, 1 H), 7.64 (ddd, $J = 1.2, 7.0, 8.2$ Hz, 1 H), 7.78 (ddd, $J = 1.4, 6.9, 8.3$ Hz, 1 H), 7.86 (d, $J = 8.4$ Hz, 1 H), 7.94 (d, $J = 8.4$ Hz, 2 H), 8.08 (d, $J = 7.6$ Hz, 1 H), 8.11 (d, $J = 0.98$ Hz, 1 H), 8.47 (d, $J = 8.2$ Hz, 2 H), 8.58 (d, $J = 8.6$ Hz, 1 H), 8.98 (d, $J = 0.78$ Hz, 1 H). Anal. ($\text{C}_{20}\text{H}_{12}\text{F}_3\text{N}_3\text{O}$): C, H, N.

8-(6-(4-(Trifluoromethyl)phenyl)pyrimidin-4-yloxy)quinoline (28a). Following method A, 8-hydroxyquinoline (0.17 g, 1.2 mmol) and **3** (0.30 g, 1.2 mmol), after purification of the crude product by silica gel chromatography (4:1 hexanes/EtOAc), provided **28a** (0.30 g, 70%) as a white solid. Mp: 155–157 °C. MS (ESI, pos. ion) m/z : 368 ($M + 1$). ^1H NMR (400 MHz, CDCl_3) δ 7.46 (dd, $J = 4.1, 8.4$ Hz, 1 H), 7.59–7.67 (m, 3 H), 7.79 (d, $J = 8.2$ Hz, 2 H), 7.83 (dd, $J = 1.6, 7.8$ Hz, 1 H), 8.23 (d, $J = 8.2$ Hz, 2 H), 8.26 (dd, $J = 1.6, 8.2$ Hz, 1 H), 8.74 (d, $J = 1.2$ Hz, 1 H), 8.85 (dd, $J = 1.8, 4.1$ Hz, 1 H). Anal. ($\text{C}_{20}\text{H}_{12}\text{F}_3\text{N}_3\text{O}$): C, H, N.

8-(6-(4-(Trifluoromethyl)phenyl)pyrimidin-4-yloxy)isoquinoline (28b). Following method A, isoquinolin-8-ol (0.060 g, 0.41 mmol) and **3** (0.12 g, 0.45 mmol), after purification of the crude product by silica gel chromatography (gradient: 20–70% EtOAc in hexane), afforded **28b** (0.094 g, 63%) as a white solid. Mp: 194–195 °C. MS (ESI, pos. ion) m/z : 368 ($M + 1$). ^1H NMR (400 MHz, DMSO- d_6) δ 7.62 (dd, $J = 0.7, 7.5$ Hz, 1 H), 7.88 (t, $J = 7.9$ Hz, 1 H), 7.95–7.99 (m, 4 H), 8.16 (d, $J = 1.0$ Hz, 1 H), 8.49 (d, $J = 8.2$ Hz, 2 H), 8.60 (d, $J = 5.7$ Hz, 1 H), 8.82 (d, $J = 1.0$ Hz, 1 H), 9.30 (s, 1 H). Anal. ($\text{C}_{20}\text{H}_{12}\text{F}_3\text{N}_3\text{O}$): C, H, N.

5-(6-(4-(Trifluoromethyl)phenyl)pyrimidin-4-yloxy)isoquinoline (28c). Following method A, isoquinolin-5-ol (0.45 g, 3.1 mmol) and **3** (0.58 g, 2.2 mmol), after purification of the crude product by recrystallization from 40% EtOAc in hexanes, afforded **28c** (0.51 g, 61%) as an off-white solid. Mp: 183–185 °C. MS (ESI, pos. ion) m/z : 368 ($M + 1$). ^1H NMR (400 MHz, DMSO- d_6) δ 7.70 (d, $J = 5.9$ Hz, 1 H), 7.73–7.83 (m, 2 H), 7.96 (d, $J = 8.4$ Hz, 2 H), 8.07–8.18 (m, 2 H), 8.49 (d, $J = 8.2$ Hz, 2 H), 8.52 (d, $J = 6.1$ Hz, 1 H), 8.79 (d, $J = 0.98$ Hz, 1 H), 9.45 (s, 1 H). Anal. ($\text{C}_{20}\text{H}_{12}\text{F}_3\text{N}_3\text{O}$): C, H, N.

5-(6-(4-(Trifluoromethyl)phenyl)pyrimidin-4-yloxy)quinoline (28d). Following method A, 5-hydroxyquinoline (0.15 g, 1.0 mmol) and **3** (0.26 g, 1.0 mmol), after purification of the crude product by silica gel chromatography (5:1 hexanes/EtOAc), provided **28d** (0.26 g, 70%) as a white solid. Mp: 159–161 °C. MS (ESI, pos. ion) m/z : 368 ($M + 1$). ^1H NMR (400 MHz, CDCl_3) δ 7.40–7.46 (m, 2 H), 7.48 (d, $J = 1.2$ Hz, 1 H), 7.80 (d, $J = 8.6$ Hz, 2 H), 7.83 (d, $J = 7.4$ Hz, 1 H), 8.13 (d, $J = 8.6$ Hz, 1 H), 8.22 (d, $J = 8.2$ Hz, 2 H), 8.25 (d, $J = 8.6$ Hz, 1 H), 8.83 (d, $J = 1.2$ Hz, 1 H), 8.99 (dd, $J = 1.8, 4.1$ Hz, 1 H). Anal. ($\text{C}_{20}\text{H}_{12}\text{F}_3\text{N}_3\text{O}$): C, H, N.

4-(6-(4-(Trifluoromethyl)phenyl)pyrimidin-4-yloxy)quinoline (28e). Following method A, quinolin-4-ol (0.20 g, 1.4 mmol) and **3** (0.32 g, 1.2 mmol), after purification of the crude product by silica gel chromatography (gradient: 0–100% EtOAc in hexanes), afforded **28e** (0.31 g, 68%) as a white solid. Mp: 209–210 °C. MS (ESI, pos. ion) m/z : 368 ($M + 1$). ^1H NMR (400 MHz, DMSO- d_6) δ 6.31 (d, $J = 8.0$ Hz, 1 H), 7.49 (ddd, $J = 0.8, 7.0, 7.8$ Hz, 1 H), 7.67 (ddd, $J = 1.6, 6.8, 8.4$ Hz, 1 H), 7.73 (d, $J = 8.4$ Hz, 1 H), 7.99 (d, $J = 8.2$ Hz, 2 H), 8.24 (dd, $J = 1.5, 7.9$ Hz, 1 H), 8.35 (d, $J = 7.8$ Hz, 1 H), 8.54 (d, $J = 8.2$ Hz, 2 H), 8.63 (s, 1 H), 9.45 (s, 1 H). Anal. ($\text{C}_{20}\text{H}_{12}\text{F}_3\text{N}_3\text{O}$): C, H, N.

4-(6-(4-(Trifluoromethyl)phenyl)pyrimidin-4-yloxy)isoquinoline (28f). Following method B, isoquinolin-4-ol (0.060 g, 0.41 mmol) and **3** (0.18 g, 0.74 mmol), after purification of the crude product by silica gel chromatography (gradient: 20–70% EtOAc in hexanes), provided **28f** (0.048 g, 32%) as a yellow solid. Mp: 206–211 °C. MS (ESI, pos. ion) m/z : 368 ($M + 1$). ^1H NMR (400 MHz, DMSO- d_6) δ 7.76–7.84 (m, 2 H), 7.85–7.89 (m, 1 H), 7.96 (d, $J = 8.2$ Hz, 2 H), 8.17 (d, $J = 1.0$ Hz, 1 H), 8.27–8.30 (m, 1 H), 8.49 (d, $J = 8.2$ Hz, 2 H), 8.55 (s, 1 H), 8.80 (d, $J = 1.2$ Hz, 1 H), 9.34 (s, 1 H). Anal. Calcd for $\text{C}_{20}\text{H}_{12}\text{F}_3\text{N}_3\text{O}$: C, 65.40; H, 3.29; N, 11.44. Found: C, 64.83; H, 3.21; N, 11.33.

1-(6-(4-(Trifluoromethyl)phenyl)pyrimidin-4-yloxy)isoquinoline (28g). Following method A, isoquinolin-1-ol (0.20 g, 1.4 mmol) and **3** (0.32 g, 1.2 mmol), after purification of the crude product by silica gel chromatography (gradient: 50–80% EtOAc in hexanes), afforded **28g** (0.17 g, 37%) as a white solid. Mp: 186–187 °C. MS (ESI, pos. ion) m/z : 368 ($M + 1$). ^1H NMR (400 MHz, DMSO- d_6) δ 6.89 (d, $J = 7.8$ Hz, 1 H), 7.63 (ddd, $J = 1.2, 6.8, 8.0$ Hz, 1 H), 7.77 (d, $J = 7.4$ Hz, 1 H), 7.84 (ddd, $J = 1.2, 6.8, 8.0$ Hz, 1 H), 7.98 (d, $J = 8.2$ Hz, 2 H), 8.03 (d, $J = 7.6$ Hz, 1 H), 8.35 (d, $J = 7.4$ Hz, 1 H), 8.44 (d, $J = 8.2$ Hz, 2 H), 8.81 (d, $J = 0.98$ Hz, 1 H), 9.39 (s, 1 H). Anal. ($\text{C}_{20}\text{H}_{12}\text{F}_3\text{N}_3\text{O}$): C, H, N.

8-[6-(4-(Trifluoromethyl)phenyl)-pyrimidin-4-yloxy]-1H-quinolin-2-one (29a). Following method D, 2,8-quinolinediol (0.075 g, 0.46 mmol) and **3** (0.10 g, 0.39 mmol) provided the crude product. The solids were filtered, washed with EtOAc, and dried in vacuo for 16 h to afford **29a** (140 mg, 94%) as long white needles. Mp: 312 °C. HRMS (TOF, pos. ion.) calcd for $\text{C}_{20}\text{H}_{13}\text{F}_3\text{N}_3\text{O}_2^+$, 384.0954; found, 384.0951. ^1H NMR (400 MHz, DMSO- d_6) δ 7.27 (dd, $J = 8.2, 9.0$ Hz, 2 H), 7.65 (t, $J = 8.2$ Hz, 1 H), 7.93 (d, $J = 8.2$ Hz, 2 H), 8.00 (s, 1 H), 8.07 (s, 1 H), 8.46 (d, $J = 8.2$ Hz, 2 H), 8.79 (s, 1 H), 12.64 (s, 1 H). Anal. ($\text{C}_{20}\text{H}_{12}\text{F}_3\text{N}_3\text{O}_2$): C, H, N, F.

2-Methoxy-8-[6-(4-trifluoromethyl-phenyl)-pyrimidin-4-yloxy]-quinoline (29b). Following method B, 2-methoxy-quinolin-8-ol (0.090 g, 0.51 mmol) and **3** (0.19 g, 0.71 mmol), after purification of the crude product by silica gel chromatography (1:9 EtOAc/hexanes), provided **29b** (0.17 g, 85%) as a white solid. Mp: 159–161 °C. MS (ESI, pos. ion) m/z : 398 ($M + 1$). ^1H NMR (400 MHz, CDCl_3) δ 3.58 (s, 3 H), 6.92 (d, $J = 8.6$ Hz, 1 H), 7.45–7.51 (m, 2 H), 7.56–7.61 (m, 1 H), 7.68–7.74 (m, 1 H), 7.80 (d, $J = 8.2$ Hz, 2 H), 8.06 (d, $J = 9.0$ Hz, 1 H), 8.22 (d, $J = 8.2$ Hz, 2 H), 8.79 (s, 1 H). Anal. ($\text{C}_{20}\text{H}_{11}\text{ClF}_3\text{N}_3\text{O}$): C, H, N.

Methyl-8-[6-(4-trifluoromethyl-phenyl)-pyrimidin-4-yloxy]-quinolin-2-yl]-amine (29c). To a solution of 2-chloroquinolin-8-ol (**5**; 0.18 g, 1 mmol) in 1,4-dioxane (3 mL) was added 2 M methylamine in THF (10 mL, 20 mmol). The reaction mixture was stirred and heated in a microwave (Smith Synthesizer, Personal Chemistry, Inc., Uppsala, Sweden) at 200 °C for 12 min. The reaction mixture was allowed to cool to room temperature, then partitioned between EtOAc and 1 N NaOH. The aqueous layer was extracted with EtOAc (3 \times), and the combined organic extracts were washed with satd NaCl, dried over Na_2SO_4 , filtered, and concentrated in vacuo. The crude product was recrystallized from MeOH/ H_2O to provide 2-methylamino-quinolin-8-ol (**6**) as a light-yellow solid (0.12 g, 71%). MS (ESI, pos. ion) m/z : 175 ($M + 1$).

Following method B, 2-methylamino-quinolin-8-ol (**6**; 0.12 g, 0.71 mmol) and **3** (0.22 g, 0.85 mmol), after purification of the crude product by silica gel chromatography (1:5 EtOAc in hexanes) and recrystallization from EtOAc in hexanes, provided **29c** (0.038 g, 14%) as a white crystalline solid. Mp: 163–165 °C. MS (ESI, pos. ion) m/z : 397 ($M + 1$). ^1H NMR (400 MHz, CDCl_3) δ 2.64 (d, $J = 4.7$ Hz, 3 H), 6.60 (d, $J = 9.0$ Hz, 1 H), 7.24–7.28 (m, 1 H), 7.44–7.48 (m, 2 H), 7.52–7.57 (m, 1 H), 7.77 (d, $J = 8.2$ Hz, 2 H), 7.83 (d, $J = 9.0$ Hz, 1 H), 8.18 (d, $J = 8.2$ Hz, 2 H), 8.79 (s, 1 H). Anal. Calcd for $\text{C}_{21}\text{H}_{15}\text{F}_3\text{N}_4\text{O}$: C, 63.63; H, 3.81; N, 14.14. Found: C, 62.98; H, 3.83; N, 13.77.

***N,N*-Dimethyl-8-(6-(4-(trifluoromethyl)phenyl)pyrimidin-4-yloxy)quinolin-2-amine (29d).** Following the same procedure described for compound **6**, 2-chloro-quinolin-8-ol (**5**; 0.18 g, 1.0 mmol) and 2 M dimethylamine in THF provided 2-(dimethylami-

no)quinolin-8-ol (**7**; 0.10 g, 56%) as a light-tan solid. MS (ESI, pos. ion) m/z : 189 ($M + 1$).

Following method B, 2-(dimethylamino)quinolin-8-ol (**7**; 0.10 g, 0.53 mmol) and **3** (0.14 g, 0.53 mmol), after purification of the crude product by silica gel chromatography (1:5 of EtOAc in hexanes) and recrystallization from EtOAc in hexanes, provided **29d** (0.050 g, 23%) as a white solid. Mp: 170–182 °C. MS (ESI, pos. ion) m/z : 411 ($M + 1$). ^1H NMR (400 MHz, CDCl_3) δ 2.87 (s, 6 H), 6.85 (d, $J = 9.2$ Hz, 1 H), 7.24 (t, $J = 8.0$ Hz, 1 H), 7.43 (d, $J = 1.2$ Hz, 1 H), 7.47 (dd, $J = 1.2, 8.0$ Hz, 1 H), 7.55 (dd, $J = 1.2, 8.0$ Hz, 1 H), 7.76 (d, $J = 8.0$ Hz, 2 H), 7.90 (d, $J = 9.2$ Hz, 1 H), 8.16 (d, $J = 8.0$ Hz, 2 H), 8.79 (d, $J = 1.0$ Hz, 1 H). Anal. ($\text{C}_{22}\text{H}_{17}\text{F}_3\text{N}_4\text{O}$): C, H, N.

8-[6-(4-Trifluoromethyl-phenyl)-pyrimidin-4-yloxy]-quinazolin-2-ylamine (30). To a room temperature solution of 3-methoxy-2-nitro-benzaldehyde (**8**; 15 g, 81 mmol) and NH_4Cl (4.4 g, 82 mmol) in 80% aq MeOH (250 mL) was added iron dust (21 g, 370 mmol). The reaction mixture was stirred at 60 °C for 2 h. After allowing to cool to room temperature, the reaction mixture was filtered through a pad of Celite. The filter cake was washed with MeOH and the combined filtrate was concentrated in vacuo to afford an aqueous mixture. The mixture was extracted with CH_2Cl_2 ($3\times$), and the combined organic layers were washed with satd NaCl, dried over Na_2SO_4 , filtered, and concentrated in vacuo. Purification of the crude product by silica gel chromatography (gradient: 0 to 20% EtOAc in hexanes) provided 2-amino-3-methoxy-benzaldehyde (**9**; 3.8 g, 31%) as a yellow oil. ^1H NMR (400 MHz, CDCl_3) δ 3.88 (s, 3 H), 6.40 (br s, 2 H), 6.68 (t, $J = 8.0$ Hz, 1 H), 6.88 (dd, $J = 1.2, 8.0$ Hz, 1 H), 7.12 (dd, $J = 1.2, 8.0$ Hz, 1 H), 9.89 (s, 1 H).

A mixture of 2-amino-3-methoxy-benzaldehyde (**9**; 3.8 g, 25 mmol), guanidine hydrochloride (4.9 g, 51 mmol), Na_2CO_3 (5.4 g, 51 mmol), and decalin (55 mL) was stirred at 190 °C for 2.5 h. The hot solution was decanted from the solids and allowed to cool to room temperature. The resultant suspension was diluted with hexane. The solid was collected by suction filtration, washed with hexane and pentane, and dried in vacuo to afford 2-amino-8-methoxyquinazoline (2.2 g, 48%) as a yellow amorphous solid. MS (ESI, pos. ion) m/z : 176 ($M + 1$). ^1H NMR (400 MHz, $\text{DMSO}-d_6$) δ 3.86 (s, 3 H), 6.87 (br s, 2 H), 7.09–7.16 (m, 2 H), 7.29–7.36 (m, 1 H), 9.05 (s, 1 H).

To a suspension of NaH (60% dispersion in mineral oil, 1.4 g, 35 mmol) in DMF (100 mL), stirred at 0 °C, was added ethanethiol (5.0 mL, 67 mmol). [Gas evolution was observed.] After the reaction mixture was allowed to warm to room temperature, 2-amino-8-methoxyquinazoline (1.5 g, 8.6 mmol) was added and the mixture was stirred at reflux for 4 h. The reaction was allowed to cool to room temperature and the solvent was removed in vacuo. The crude residue was azeotroped in vacuo with H_2O and purified by silica gel chromatography (gradient: 0–50% 2 M NH_3 in MeOH/ CH_2Cl_2) to give 2-amino-8-hydroxyquinazoline (**10**; 500 mg, 58%) as a pale-green amorphous solid. MS (ESI, pos. ion) m/z : 162 ($M + 1$). ^1H NMR (400 MHz, $\text{DMSO}-d_6$) δ 6.72 (br s, 2 H), 7.02–7.07 (m, 2 H), 7.21–7.26 (m, 1 H), 9.05 (s, 1 H), 9.19 (s, 1 H).

Following method D, 2-amino-8-hydroxyquinazoline (**10**; 220 mg, 1.3 mmol) and **3** (390 mg, 1.5 mmol), after purification of the crude product by silica gel chromatography (gradient: 0–40% EtOAc in hexanes) and a second purification by silica gel chromatography (gradient: 0–5% 2 M NH_3 in MeOH/ CH_2Cl_2), afforded **30** (110 mg, 22%) as a white solid. Mp: 251–253 °C. MS (ESI, pos. ion) m/z : 384.1 ($M + 1$). ^1H NMR (400 MHz, CDCl_3) δ 5.17 (s, 2 H), 7.35 (t, $J = 8.0$ Hz, 1 H), 7.54 (d, $J = 0.8$ Hz, 1 H), 7.59 (dd, $J = 1.6, 7.6$ Hz, 1 H), 7.69 (dd, $J = 1.6, 8.0$ Hz, 1 H), 7.79 (d, $J = 8.0$ Hz, 2 H), 8.22 (d, $J = 8.0$ Hz, 2 H), 8.77 (d, $J = 0.8$ Hz, 1 H), 9.10 (s, 1 H). Anal. ($\text{C}_{19}\text{H}_{12}\text{F}_3\text{N}_5\text{O}$): C, H, N.

8-[6-(4-Trifluoromethyl-phenyl)-pyrimidin-4-yloxy]-quinoxalin-2-ylamine (31). A mixture of 2-amino-3-nitrophenol (**11**; 25 g, 160 mmol) and K_2CO_3 (27 g, 195 mmol) in DMF (65 mL) was stirred at room temperature for 1 h. Methyl iodide (12 mL, 195 mmol) was added, and the reaction was stirred at room temperature

for 30 h. The reaction mixture was diluted with H_2O and extracted with EtOAc ($3\times$). The combined organic extract was dried over Na_2SO_4 , filtered, and concentrated in vacuo. The resulting dark red solid was recrystallized from hexanes to yield 2-methoxy-6-nitrobenzenamine (24 g, 87%) as orange needles. MS (ESI, pos. ion) m/z : 169 ($M + 1$). ^1H NMR (400 MHz, CDCl_3) δ 3.94 (s, 3 H), 6.46 (s, 2 H), 6.63 (dd, $J = 7.8, 8.2$ Hz, 1 H), 6.91 (d, $J = 7.8$ Hz, 1 H), 7.75 (dd, $J = 1.2, 8.6$ Hz, 2 H).

A mixture of 2-methoxy-6-nitrobenzenamine (4.6 g, 27 mmol), iron powder (11 g, 190 mmol), EtOH (130 mL), and H_2O (10 mL) was stirred at 50 °C. A solution of 12 M aq HCl (1.7 mL) was added to the reaction mixture, dropwise with stirring. The reaction mixture was stirred at reflux for 3 h then allowed to cool to room temperature. The reaction mixture was neutralized with 1 N NaOH and filtered through Celite. The filtrate was concentrated in vacuo to afford a residue. The residue was partitioned between CH_2Cl_2 and satd aq NaHCO_3 . The aqueous phase was extracted with CH_2Cl_2 ($3\times$) and the combined organic layers were concentrated in vacuo. The residue was dissolved in EtOH (30 mL) and treated with concd H_2SO_4 until no more precipitate was formed. The precipitate was collected by suction filtration, washed with EtOH, and dried in vacuo for 20 h at room temperature to afford 3-methoxy-benzene-1,2-diamine hydrogen sulfate salt (**12**; 6.3 g, 97%) as an off-white powder. MS (ESI, pos. ion) m/z : 139 ($M - \text{HSO}_4^-$). ^1H NMR (400 MHz, D_2O) δ 3.84 (s, 3 H), 6.82 (dd, $J = 1.2, 8.2$ Hz, 1 H), 6.93 (dd, $J = 1.2, 8.6$ Hz, 1 H), 7.21 (t, $J = 8.2$ Hz, 1 H).

A solution of 3-methoxy-benzene-1,2-diamine hydrogen sulfate salt (**12**; 4.1 g, 17 mmol) in EtOH (21 mL) and H_2O (48 mL) was neutralized by careful addition of solid NaHCO_3 . The mixture was treated with ethyl glyoxylate solution (50% in toluene, 3.8 mL, 19 mmol) then stirred at reflux for 1 h. The reaction was allowed to cool to room temperature and partitioned between satd aq NH_4Cl and 25% i -PrOH/ CHCl_3 . The aqueous layer was extracted with 25% i -PrOH/ CHCl_3 ($3\times$). The combined organic layers were dried over Na_2SO_4 , filtered, and concentrated in vacuo. Silica gel chromatography of the crude residue (gradient: 0–2.5% MeOH/ CH_2Cl_2) afforded two products. (1) 8-Methoxy-1H-quinoxalin-2-one (**13**; 1.1 g, 37%) as an off-white powder. MS (ESI, pos. ion) m/z : 177 ($M + 1$). ^1H NMR (400 MHz, CDCl_3) δ 4.01 (s, 3 H), 7.03 (d, $J = 8.2$ Hz, 1 H), 7.26 (t, $J = 8.2$ Hz, 1 H), 7.49 (dd, $J = 1.2, 8.2$ Hz, 1 H), 8.32 (s, 1 H), 9.28 (s, 1 H). (2) 5-Methoxy-1H-quinoxalin-2-one (0.82 g, 27%) as an off-white powder. MS (ESI, pos. ion) m/z : 177 ($M + 1$). ^1H NMR (400 MHz, CDCl_3) δ 4.06 (s, 3 H), 6.82 (d, $J = 7.4$ Hz, 1 H), 6.95 (dd, $J = 0.8, 8.2$ Hz, 1 H), 7.51 (t, $J = 8.2$ Hz, 1 H), 8.33 (s, 1 H), 12.22 (s, 1 H).

A mixture of 8-methoxy-1H-quinoxalin-2-one (**13**; 0.62 g, 3.5 mmol) and POCl_3 (6.0 mL, 64 mmol) was stirred at 105 °C in an oil bath for 4 h. The reaction mixture was allowed to cool to room temperature and the excess POCl_3 was removed by vacuum distillation. The residue was partitioned between satd aq NaHCO_3 and CH_2Cl_2 and stirred for 3 h to quench residual POCl_3 . The aqueous layer was extracted with CH_2Cl_2 ($3\times$). The combined organic extract was dried over Na_2SO_4 and filtered through a pad of silica gel, eluting with EtOAc. The filtrate was concentrated in vacuo to afford 2-chloro-8-methoxyquinoxaline (0.66 g, 97%) as a tan solid. MS (ESI, pos. ion) m/z : 195 ($M + 1$). ^1H NMR (400 MHz, CDCl_3) δ 4.10 (s, 3 H), 7.16 (dd, $J = 3.6, 5.6$ Hz, 1 H), 7.71 (d, $J = 3.6$ Hz, 1 H), 7.71 (d, $J = 5.6$ Hz, 1 H), 8.80 (s, 1 H).

A mixture of 2-chloro-8-methoxyquinoxaline (0.42 g, 2.2 mmol) and CuI (0.21 g, 1.1 mmol) in 28–30% NH_4OH (1.5 mL) was stirred and heated in a microwave (Smith Synthesizer, Personal Chemistry, Inc., Uppsala, Sweden) at 140 °C for 10 min. The reaction mixture was diluted with H_2O and the solids were collected by suction filtration and washed with copious amounts of H_2O . The solid was dried in vacuo for 20 h at room temperature to afford 8-methoxyquinoxalin-2-ylamine (0.27 g, 70%) as a brown powder. MS (ESI, pos. ion) m/z : 176 ($M + 1$). ^1H NMR (400 MHz, $\text{DMSO}-d_6$) δ 3.88 (s, 3 H), 6.98 (s, 2 H), 7.04 (d, $J = 8.0$ Hz, 1 H), 7.24 (t, $J = 8.0$ Hz, 1 H), 7.34 (d, $J = 8.4$ Hz, 1 H), 8.27 (s, 1 H).

To a suspension of 8-methoxyquinoxalin-2-ylamine (0.12 g, 0.68 mmol) in benzene (10 mL) was added AlCl_3 (0.82 g, 6.2 mmol), and the mixture was stirred at reflux for 2 h. The reaction was allowed to cool to room temperature and quenched by careful addition of satd aq NaHCO_3 . The resulting mixture was extracted with 25% *i*-PrOH/ CHCl_3 (5 \times). The combined organic extract was dried over Na_2SO_4 , filtered, and concentrated in vacuo. Purification of the crude residue by silica gel chromatography (gradient: 0–7.5% MeOH/ CH_2Cl_2) afforded 3-aminoquinoxalin-5-ol (**14**; 0.050 g, 46%) as a brown powder. MS (ESI, pos. ion) m/z : 162 ($M + 1$). ^1H NMR (400 MHz, $\text{DMSO}-d_6$) δ 6.83 (s, 2 H), 6.94 (dd, $J = 1.2, 7.4$ Hz, 1 H), 7.14 (t, $J = 8.0$ Hz, 1 H), 7.24 (dd, $J = 1.4, 8.4$ Hz, 1 H), 8.29 (s, 1 H), 9.13 (s, 1 H).

Following method D, 3-aminoquinoxalin-5-ol (**14**; 0.069 g, 0.43 mmol) and **3** (0.13 g, 0.51 mmol), after purification of the crude product by silica gel chromatography (gradient: 0–75% EtOAc in hexanes), afforded **31** (0.11 g, 66%) as an off-white powder. Mp: 214–216 °C. HRMS (TOF, pos. ion.) calcd for $\text{C}_{19}\text{H}_{13}\text{F}_3\text{N}_5\text{O}^+$, 384.1067; found, 384.1063. ^1H NMR (400 MHz, CDCl_3) δ 4.95 (s, 2 H), 7.49 (m, 3 H), 7.78 (d, $J = 8.4$ Hz, 2 H), 7.91 (dd, $J = 2.4, 6.8$ Hz, 1 H), 8.20 (d, $J = 8.4$ Hz, 2 H), 8.32 (s, 1 H), 8.77 (s, 1 H). Anal. Calcd for $\text{C}_{19}\text{H}_{12}\text{F}_3\text{N}_5\text{O}$: C, 59.53; H, 3.16; F, 14.87; N, 18.27. Found: C, 58.26; H, 3.24; F, 14.25; N, 17.63.

3-Amino-5-(6-(4-(trifluoromethyl)phenyl)pyrimidin-4-yloxy)-quinoxalin-2(1H)-one (32). To a suspension of 3-methoxybenzene-1,2-diamine hydrogen sulfate salt (**12**; 2.4 g, 10 mmol) in EtOH (15 mL) and H_2O (1 mL) was added solid NaHCO_3 (1.7 g, 20 mmol). When gas evolution was complete, ethoxy-imino-acetic acid ethyl ester¹⁴ (**15**; 1.6 g, 11 mmol) was added, and the mixture was stirred at room temperature for 16 h. The reaction mixture was diluted with satd aq NaHCO_3 and extracted with 25% *i*-PrOH/ CHCl_3 (5 \times). The combined organic extract was dried over Na_2SO_4 , filtered, and concentrated in vacuo. Purification of the residue by silica gel chromatography (gradient: 0–5% MeOH/ CH_2Cl_2) afforded two products: (1) 3-Amino-5-methoxy-1H-quinoxalin-2-one (**16**; 0.44 g, 23%) as a light brown powder. MS (ESI, pos. ion) m/z : 192 ($M + 1$). ^1H NMR (400 MHz, $\text{DMSO}-d_6$) δ 3.81 (s, 3 H), 6.73 (d, $J = 8.6$ Hz, 1 H), 6.75 (d, $J = 8.2$ Hz, 1 H), 7.04 (t, $J = 8.2$ Hz, 1 H), 7.04 (br s, 2 H), 12.08 (s, 1 H). (2) 3-Amino-8-methoxy-1H-quinoxalin-2-one (**17**; 0.75 g, 39%) as a pale brown powder. MS (ESI, pos. ion) m/z : 192 ($M + 1$). ^1H NMR (400 MHz, $\text{DMSO}-d_6$) δ 3.86 (s, 3 H), 6.79 (d, $J = 7.8$ Hz, 1 H), 6.90 (d, $J = 7.8$ Hz, 1 H), 7.05 (t, $J = 8.0$ Hz, 1 H), 7.07 (s, 2 H), 11.51 (s, 1 H).

To a suspension of 3-amino-5-methoxy-1H-quinoxalin-2-one (**16**; 0.47 g, 2.5 mmol) in benzene (25 mL) was added AlCl_3 (0.97 g, 7.4 mmol), and the mixture was stirred at reflux for 2 h. The reaction was quenched by careful addition of satd aq NaHCO_3 and extracted with 25% *i*-PrOH/ CHCl_3 (5 \times). The combined organic extract was dried over Na_2SO_4 , filtered, and concentrated in vacuo to afford 3-amino-5-hydroxy-1H-quinoxalin-2-one (**18**; 0.34 g, 78%) as a brown powder. MS (ESI, pos. ion) m/z : 178 ($M + 1$). ^1H NMR (400 MHz, $\text{DMSO}-d_6$) δ 6.58 (dd, $J = 1.2, 7.8$ Hz, 1 H), 6.60 (dd, $J = 1.2, 8.2$ Hz, 1 H), 6.89 (s, 2 H), 6.92 (dd, $J = 7.8, 8.2$ Hz, 1 H), 8.81 (s, 1 H), 12.04 (s, 1 H).

Following method C, 3-amino-5-hydroxy-1H-quinoxalin-2-one (**18**; 0.33 g, 1.9 mmol) and **3** (0.49 g, 1.9 mmol), after purification of the crude product by silica gel chromatography (gradient: 0–2.5% 2 M NH_3 in MeOH/ CH_2Cl_2), afforded **32** (0.28 g, 38%) as an off-white solid. Mp: 334–335 °C (dec). HRMS (TOF, pos. ion) calcd for $\text{C}_{19}\text{H}_{13}\text{F}_3\text{N}_5\text{O}_2^+$, 400.1016; found, 400.1012. ^1H NMR (400 MHz, $\text{DMSO}-d_6$) δ 7.03 (d, $J = 7.6$ Hz, 1 H), 7.10 (d, $J = 6.8$ Hz, 1 H), 7.12 (br s, 2 H), 7.16 (t, $J = 8.0$ Hz, 1 H), 7.85 (s, 1 H), 7.91 (d, $J = 8.4$ Hz, 2 H), 8.43 (d, $J = 8.4$ Hz, 2 H), 8.78 (s, 1 H), 12.30 (s, 1 H). Anal. Calcd for $\text{C}_{19}\text{H}_{12}\text{F}_3\text{N}_5\text{O}_2 \cdot 1.75\text{H}_2\text{O}$: C, 52.97; H, 3.63; F, 13.23; N, 16.25. Found: C, 53.07; H, 3.61; F, 13.00; N, 16.20. HPLC analysis, method B: 95.9% at 215 nm; 96.7% at 254 nm; retention time 5.67 min.

3-Amino-8-(6-(4-(trifluoromethyl)phenyl)pyrimidin-4-yloxy)-quinoxalin-2(1H)-one (33). Following the method described for the preparation of compound **18**, 3-amino-8-methoxy-1H-quinox-

alin-2-one (**17**; 0.75 g, 3.9 mmol) was demethylated to provide 3-amino-8-hydroxy-1H-quinoxalin-2-one (**19**). MS (ESI, pos. ion) m/z : 178 ($M + 1$). ^1H NMR (400 MHz, D_2O) δ 6.71 (d, $J = 8.2$ Hz, 1 H), 6.79 (d, $J = 8.2$ Hz, 1 H), 7.22 (t, $J = 8.0$ Hz, 1 H).

Following method D, 3-amino-8-hydroxy-1H-quinoxalin-2-one (**19**; 0.69 g, 3.9 mmol) and **3** (1.0 g, 3.9 mmol), after purification of the crude product by silica gel chromatography (gradient: 0–2.5% MeOH in CH_2Cl_2), afforded **33** (0.42 g, 27%) as a white powder. Mp: 288 °C. HRMS (TOF, pos. ion) calcd for $\text{C}_{19}\text{H}_{13}\text{F}_3\text{N}_5\text{O}_2^+$, 400.1016; found, 400.1015. ^1H NMR (400 MHz, $\text{DMSO}-d_6$) δ 7.03 (d, $J = 8.0$ Hz, 1 H), 7.16 (t, $J = 8.0$ Hz, 1 H), 7.20 (br s, 2 H), 7.24 (d, $J = 8.0$ Hz, 1 H), 7.93 (s, 1 H), 7.95 (d, $J = 8.4$ Hz, 2 H), 8.46 (d, $J = 8.0$ Hz, 2 H), 8.81 (s, 1 H), 12.11 (s, 1 H). Anal. ($\text{C}_{19}\text{H}_{12}\text{F}_3\text{N}_5\text{O}_2$): C, H, N, F.

Acknowledgment. The authors thank Paul Reider, Randy Hungate, Jean-Claude Louis, and Chris Fibiger for their support of this research program. Thanks go to James Davis, Gal Hever, Rongzhen Kuang, Jue Wang, Dawn Zhu, and Shoushu Jiao for conducting the in vivo pharmacology studies and to Nuria Tamayo for helpful discussions regarding the SAR in this series. Finally, we acknowledge all of our colleagues on the TRPV1 research team (pharmaceutics, toxicology, PKDM, process research and development, analytical support, medical sciences) who helped advance AMG 517 forward into development, with special thanks to Annette Bak and David Hovland.

Supporting Information Available: Combustion analysis results for final compounds **21–26**, **27a–f**, **28a–g**, **29a–d**, and **30–33**. This material is available free of charge via the Internet at <http://pubs.acs.org>.

References

- (1) (a) Appendino, G.; Munoz, E.; Fiebich, B. L. TRPV1 (Vanilloid receptor, Capsaicin receptor) Agonists and Antagonists. *Expert Opin. Ther. Pat.* **2003**, *13*, 1825–1837. (b) Rami, K. H.; Gunthorpe, M. J. The Therapeutic Potential of TRPV1 (VR1) Antagonists: Clinical Answers Await. *Drug Discovery Today* **2004**, *1*, 97–104. (c) Breitenbucher, G.; Chaplan, S. R.; Carrutgers, N. I. The TRPV1 Vanilloid Receptor: A Target for Therapeutic Intervention. In *Ann. Rep. Med. Chem.*; Doherty, A. M., Ed.; Elsevier Inc.: San Diego, 2005; Vol. 40, pp 185–198.
- (2) Norman, M. H.; Fotsch, C.; Doherty, E. M.; Bo, Y.; Chen, N.; Chakrabarti, P.; Gavva, N. R.; Nishimura, N.; Nixey, T.; Ognyanov, V. I.; Rzasas, R.; Stec, M.; Surapaneni, S.; Tamir, R.; Viswanadhan, V.; Zhu, J.; Treanor, J. J. S. Novel Vanilloid Receptor-1 Antagonists: 1. Conformationally Restricted Analogues of *trans*-Cinnamides. *J. Med. Chem.* **2007**, *50*, 3497–3514.
- (3) Chakrabarti, P. P.; Chen, N.; Doherty, E. M.; Dominguez, C.; Falsey, J. R.; Fotsch, C. H.; Hulme, C.; Katon, J.; Nixey, T.; Norman, M. H.; Ognyanov, V. I.; Pettus, L. H.; Rzasas, R. M.; Stec, M.; Wang, H.-L.; Zhu, J. (Amgen Inc.) Preparation of (aryloxy)pyrimidine and (aryloxy)pyridazine as vanilloid receptor ligands. WO 04014871, 2004.
- (4) Csikos, E.; Gonczi, C.; Podanyi, B.; Toth, G.; Hermecz, I. Regioselectivity in preparation of unsymmetrically substituted 3-aminoquinoxalin-2(1H)-ones. *J. Chem. Soc., Perkin Trans. 1* **1999**, *13*, 1789–1793.
- (5) Doherty, E. M.; Fotsch, C.; Bo, Y.; Chakrabarti, P. P.; Chen, N.; Gavva, N.; Han, N.; Kelly, M. G.; Kincaid, J.; Klionsky, L.; Liu, Q.; Ognyanov, V. I.; Tamir, R.; Wang, X.; Zhu, J.; Norman, M. H.; Treanor, J. J. S. Discovery of Potent, Orally Available Vanilloid Receptor-1 Antagonists. Structure-Activity Relationship of *N*-Aryl Cinnamides. *J. Med. Chem.* **2005**, *48* (1), 71–90.
- (6) This observation is also consistent with the results of 6,6-fused heteroaromatic-containing urea TRPV1 antagonists reported by Gomtsyan, A.; Bayburt, E. K.; Schmidt, R. G.; Zheng, G. Z.; Perner, R. J.; Didomenico, S.; Koenig, J. R.; Turner, S.; Jinkerson, T.; Drizin, I.; Hannick, S. M.; Macri, B. S.; McDonald, H. A.; Honore, P.; Wismer, C. T.; Marsh, K. C.; Wetter, J.; Stewart, K. D.; Oie, T.; Jarvis, M. F.; Surowy, C. S.; Faltny, C. R.; Lee, C.-H. Novel Transient Receptor Potential Vanilloid 1 Receptor Antagonists for the Treatment of Pain: Structure-Activity Relationships for Ureas with Quinoline, Isoquinoline, Quinazoline, Phthalazine, Quinoxaline, and Cinnoline Moieties. *J. Med. Chem.* **2005**, *48* (3), 744–752.

- (7) The effect on in vitro potency for these antagonists as a result of varying pH is beyond the scope of this discussion, but will be presented in more detail in a subsequent article.
- (8) Gavva, N. R.; Tamir, R.; Qu, Y.; Klionsky, L.; Zhang, T. J.; Immke, D.; Wang, J.; Zhu, D.; Vanderah, T. W.; Porreca, F.; Doherty, E. M.; Norman, M. H.; Wild, K. D.; Bannon, A. W.; Louis, J.-C.; Treanor, J. J. S. AMG 9810 [(E)-3-(4-*t*-Butylphenyl)-*N*-(2,3-dihydrobenzo[*b*][1,4]dioxin-6-yl)acrylamide], a Novel Vanilloid Receptor 1 (TRPV1) Antagonist with Antihyperalgesic Properties. *J. Pharmacol. Exp. Ther.* **2005**, 313, 474–484.
- (9) Lewis, F. D.; Reddy, G. D.; Elbert, J. E.; Tillberg, B. E.; Meltzer, J. A.; Kojima, M. Lewis Acid Catalysis of Photochemical Reactions. 10. Spectroscopy and Photochemistry of 2-Quinolones and their Lewis Acid Complexes. *J. Org. Chem.* **1991**, 56 (18), 5311–5318.
- (10) Compound **20** was incubated at a concentration of 10 μ M with rat or human hepatocytes (1 million cells/mL) for 4 h at 37 °C. Control incubations in the absence of cells were also carried out. Reactions were quenched with acetonitrile containing 0.05% formic acid. The supernatant was analyzed by reverse phase (YMC ODS-AQ, 4.6 \times 250mm, 5 μ m) HPLC-MS/MS with radiometric detection and ion trap mass spectrometry using electrospray ionization. Hydrolysis experiments were conducted with glucuronidase and/or sulfatase to confirm the presence of glucuronide and/or sulfate metabolites.
- (11) Stevens, J. R.; Pfister, K.; Wolf, F. J. Substituted Sulfaquinoxalines. I. The Isolation and Synthesis of 3-Hydroxy-2-sulfanilamidoquinoxaline and of Related Quinoxalines *J. Am. Chem. Soc.* **1946**, 68 (6), 1035–1039.
- (12) Tan, H.; Semin, D.; Wacker, M.; Cheetham, J. An Automated Screening Assay for Determination of Aqueous Equilibrium Solubility Enabling SPR Study During Drug Lead Optimization. *JALA* **2005**, 10 (6), 364–373.
- (13) Gavva, N. R.; Bannon, A. W.; Immke, D. C.; Tamir, R.; Klionsky, L.; Hever, G.; Wang, J.; Davis, J.; Zajic, G.; Arik, L.; Shi, L.; Bak, A.; Surapaneni, S.; Hovland, D. N., Jr.; Louis, J.-C.; Norman, M. H.; Magal, E.; Treanor, J. J. S. Preclinical Pharmacology of AMG 517: A Novel TRPV1 Antagonist in the Clinic, Society for Neuroscience annual meeting, Atlanta, GA, 2006, poster no. 51.21/M13.
- (14) McKillop, A.; Chattopadhyay, S. K.; Henderson, A.; Avendano, C. Applications of Ethyl Carboethoxyformimidate to Heterocyclic Synthesis. Preparation of Condensed Pyrazinones and 1,4-Oxazinones. *Synthesis* **1997**, 3, 301–304.

JM070190P